



doi:10.1016/S0016-7037(00)01375-3

## Theoretical estimates of equilibrium chlorine-isotope fractionations

EDWIN A. SCHAUBLE,\* GEORGE R. ROSSMAN, and H. P. TAYLOR, JR.

Division of Geological and Planetary Sciences, MC100-23, California Institute of Technology, Pasadena, CA 91125, USA

(Received June 10, 2002; accepted in revised form November 19, 2002)

**Abstract**—Equilibrium chlorine-isotope ( $^{37}\text{Cl}/^{35}\text{Cl}$ ) fractionations have been determined by using published vibrational spectra and force-field modeling to calculate reduced partition function ratios for Cl-isotope exchange. Ab initio force fields calculated at the HF/6-31G(d) level are used to estimate unknown vibrational frequencies of  $^{37}\text{Cl}$ -bearing molecules, whereas crystalline phases are modeled by published lattice-dynamics models. Calculated fractionations are principally controlled by the oxidation state of Cl and its bond partners. Molecular mass (or the absence of C-H bonds) also appears to play a role in determining relative fractionations among simple Cl-bearing organic species. Molecules and complexes with oxidized Cl (i.e.,  $\text{Cl}^0$ ,  $\text{Cl}^+$ , etc.) will concentrate  $^{37}\text{Cl}$  relative to chlorides (substances with  $\text{Cl}^-$ ). At 298 K,  $\text{ClO}_2$  (containing  $\text{Cl}^{4+}$ ) and  $[\text{ClO}_4]^-$  (containing  $\text{Cl}^{7+}$ ) will concentrate  $^{37}\text{Cl}$  relative to chlorides by as much as 27‰ and 73‰, respectively, in rough agreement with earlier calculations. Among chlorides,  $^{37}\text{Cl}$  will be concentrated in substances where Cl is bonded to +2 cations (i.e.,  $\text{FeCl}_2$ ,  $\text{MnCl}_2$ , micas, and amphiboles) relative to substances where Cl is bonded to +1 cations (such as  $\text{NaCl}$ ) by ~2 to 3‰ at 298 K; organic molecules with C-Cl bonds will be even richer in  $^{37}\text{Cl}$  (~5 to 9‰ at 298 K). Precipitation experiments, in combination with our results, provide an estimate for Cl-isotope partitioning in brines and suggest that silicates (to the extent that their Cl atoms are associated with nearest-neighbor +2 cations analogous with  $\text{FeCl}_2$  and  $\text{MnCl}_2$ ) will have higher  $^{37}\text{Cl}/^{35}\text{Cl}$  ratios than coexisting brine (by ~2 to 3‰ at room temperature). Calculated fractionations between  $\text{HCl}$  and  $\text{Cl}_2$ , and between brines and such alteration minerals, are in qualitative agreement with both experimental results and systematics observed in natural samples. Our results suggest that Cl-bearing organic molecules will have markedly higher  $^{37}\text{Cl}/^{35}\text{Cl}$  ratios (by 5.8‰ to 8.5‰ at 295 K) than coexisting aqueous solutions at equilibrium. Predicted fractionations are consistent with the presence of an isotopically heavy reservoir of  $\text{HCl}$  that is in exchange equilibrium with  $\text{Cl}^-_{\text{aq}}$  in large marine aerosols. Copyright © 2003 Elsevier Ltd

### 1. INTRODUCTION

The purpose of this study is to provide estimates of equilibrium chlorine-isotope fractionations among a variety of geochemically interesting species. Substances studied include crystalline alkali-chloride salts,  $\text{FeCl}_2$ , and  $\text{MnCl}_2$  (as analogs for Cl-bearing silicate minerals), in addition to gas-phase molecules and dissolved species. Although chlorine was one of the first isotopic systems to be investigated theoretically (Urey and Greiff, 1935; Urey, 1947), major gaps still exist in our understanding of chlorine-isotope partitioning in minerals, solutions, and organic molecules. Improved knowledge of equilibrium chlorine-isotope partitioning behavior should lead to greater progress in understanding the planetary chlorine cycle, groundwater processes, atmospheric chemistry, and the sources and fate of chlorine-containing pollutants. We have focused on simple, well-studied, and abundant molecular and crystalline phases that are either of direct relevance to areas of current or possible future research in Cl-isotope geochemistry (i.e.,  $\text{NaCl}$ ,  $\text{C}_2\text{HCl}_3$ ) or are illustrative of the chemical systematics controlling equilibrium Cl-isotope fractionation (i.e.,  $\text{NaCl}$  vs.  $\text{RbCl}$ ). However, our ability to model Cl-isotope fractionations is often limited by the need for accurate vibrational frequencies for at least one isotopic form of every modeled substance, and by the need to calculate unknown frequencies of  $^{37}\text{Cl}$ -bearing species. Because of these limitations, some substances of obvious importance (such as  $\text{Cl}^-$  in aqueous solution, Cl-bearing silicates,

and crystalline  $\text{NH}_4\text{Cl}$ ), as well as solution effects for molecular species, are not directly modeled in the present work. Instead, model Cl-isotope fractionations among alkali chloride crystals are combined with measured crystal-solution fractionations (Eggenkamp et al., 1995) to estimate the Cl-isotope partitioning behavior of saturated brines; in the absence of more model or experimental data, this estimate may also serve as a crude estimate of Cl-isotope partitioning for dissociated  $\text{Cl}^-_{\text{aq}}$  in other systems (such as seawater, meteoric waters, and dilute  $\text{HCl}$  solutions). Cl-isotope fractionations between intact molecules in solution can be related to our gas-phase models if the relevant vapor-solution fractionations are known. Equilibrium vapor-solution fractionations (i.e.,  $\text{CH}_3\text{Cl}_{\text{aq}}$  vs.  $\text{CH}_3\text{Cl}_{\text{vapor}}$ ) are often much easier to measure than the equilibrium fractionations between different gas-phase or aqueous species, particularly at low temperatures, so our models should be of use in extending experimental results for ambient near-surface and atmospheric conditions.

Chlorine has two stable isotopes,  $^{35}\text{Cl}$  and  $^{37}\text{Cl}$ , with  $^{37}\text{Cl}/^{35}\text{Cl} \approx 0.320$  (Parrington et al., 1996). Chlorine isotope ratios have been measured by both thermal-ionization and gas-source mass spectrometry (Xiao and Zhang, 1992; Long et al., 1993), and small variations have been detected in natural terrestrial samples. These variations are reported in terms of  $\delta^{37}\text{Cl}_X = 10^3 \cdot (R_X/R_{\text{standard}} - 1)$ , where  $R_X$  and  $R_{\text{standard}}$  are the  $^{37}\text{Cl}/^{35}\text{Cl}$  ratios in substance  $X$  and seawater, respectively. The observed terrestrial variation in  $\delta^{37}\text{Cl}$  is approximately +7‰ to -8‰ (Magenheim et al., 1995; Ransom et al., 1995), although larger deviations have been reported (Vengosh et al., 1989).

\* Author to whom correspondence should be addressed (edwin@gps.caltech.edu).

The highest  $^{37}\text{Cl}/^{35}\text{Cl}$  ratios are found in mid-ocean ridge basalts and Cl-bearing silicates (Magenheim et al., 1995), whereas the lowest ratios are found in pore waters from the Nankai subduction zone (Ransom et al., 1995). Groundwaters, evaporites, and organochloride pollutants also show significant deviations from the seawater ratio (Kaufmann et al., 1984; Jendrzewski et al., 2001).

Naturally formed chloride minerals, such as halite (NaCl), sylvite (KCl), and chloride-bearing silicates, have been extensively studied (Eggenkamp et al., 1995; Eastoe et al., 1999). Experimental studies have been conducted to determine equilibrium chlorine-isotope fractionations between halite, sylvite, bischofite ( $\text{MgCl}_2 \cdot 6\text{H}_2\text{O}$ ), and their saturated aqueous solutions at  $\sim 22^\circ\text{C}$  (Hoering and Parker, 1961; Eggenkamp et al., 1995). No equivalent attempts have yet been carried out for  $\text{Cl}^-$ -bearing silicates.

Equilibrium stable isotope fractionations arise mainly from small differences in the vibrational energies of isotopically light and heavy substances (Urey, 1947; Richet et al., 1977). Isotopically heavy substances vibrate at lower frequencies than their isotopically lighter equivalents, causing their vibrational energy to be slightly lower; the energy decrease caused by isotopic substitution varies from one substance to another, and is generally largest in strongly bonded substances. This variability means that there is a small energy change associated with isotopic exchange between two different substances, causing unequal partitioning of the isotopes between those substances when they are at equilibrium. Isotope partitioning in a substance is typically expressed in terms of a  $\beta$ -factor (i.e.,  $\beta_{37-35}$  for  $^{37}\text{Cl}$ - $^{35}\text{Cl}$  exchange), defined as the ratio at equilibrium of the isotope ratio of the substance of interest to the isotope ratio of dissociated atoms. In the present study,  $\beta$  is equivalent to the factor  $(s/s')$  as defined by Bigeleisen and Mayer (1947). It is convenient to report results as reduced partition function ratios (i.e.,  $1000 \cdot \ln\beta$ ), because  $1000 \cdot \ln(\beta_{37-35}[X]) - 1000 \cdot \ln(\beta_{37-35}[Y]) \approx \delta^{37}\text{Cl}_X - \delta^{37}\text{Cl}_Y$  at equilibrium.

## 2. METHODS

### 2.1. Theory

Equilibrium chlorine-isotope fractionation factors are calculated by the standard thermodynamic, quantum mechanical approach (Urey, 1947). In general, we have chosen not to consider fractionation effects arising from vibrational anharmonicity and rotation. This is done for the sake of consistency because (1) anharmonic parameters are only known for a few of the gas-phase molecules studied here, and because (2) rotational quanta are so small that they have negligible effects on equilibrium isotope partitioning at the temperatures of interest. A good example is HCl, which has a relatively large anharmonicity of  $\sim 2\%$  and by far the largest rotational quanta of the molecules studied here. Our harmonic, vibration-only model for chlorine isotope partitioning in HCl gives results within 0.3‰ of the model of Richet et al. (1977) from  $0^\circ\text{C}$  to  $1000^\circ\text{C}$ , even though the Richet et al. (1977) model takes account of quantized rotations and anharmonicity.

Excellent spectroscopic data are available for many chlorine-containing molecules, dissolved species, and a handful of minerals and crystalline compounds. Gas-phase and matrix-isolation spectra of small molecules typically resolve frequencies of both the  $^{35}\text{Cl}$ -end-member composition and one or more  $^{37}\text{Cl}$ -containing isotopomers, greatly facilitating the calculation of reduced partition function ratios. For most species, however, available spectroscopic data are incomplete, and it is necessary to calculate some or all of the vibrational frequencies of the  $^{37}\text{Cl}$ -bearing form.

In the case of a simple molecule like  $\text{Cl}_2$ , it is a straightforward exercise to calculate the vibrational frequencies of  $^{35}\text{Cl}^{37}\text{Cl}$  or  $^{37}\text{Cl}_2$  from the observed frequency for  $^{35}\text{Cl}_2$ . For more complex molecules and condensed phases, however, it is usually necessary to create a model of the forces acting on each atom. In a previous article (Schauble et al., 2001), we used a simple Urey-Bradley force field fitted to the known frequencies of each molecular complex. This procedure seems to work well for small, highly symmetric molecules and complexes where the number of independent force-field parameters is smaller than the number of observed frequencies. For more complex molecules, this empirical force-field approach becomes cumbersome and less accurate.

### 2.2. Modeling Molecules

An alternative approach for molecules is to use ab initio methods to determine the force field. Ab initio force fields have the advantage that the calculated molecular structures and vibrational frequencies are not derived from observed structures and vibrational frequencies, so the suitability of the ab initio model can be independently verified by comparing it to experimental evidence. We use ab initio force fields for all molecules in this study for which isotopically substituted vibrational frequencies have not been measured or are incomplete. Harmonic molecular force fields are calculated at the Hartree-Fock level using the 6-31G(d) basis set, hereafter abbreviated HF/6-31G(d). Calculations were performed via the Macintosh version (Brett Bode, <http://www.msg.ameslab.gov/GAMESS/dist.mac.shtml>) of the GAMESS (US) quantum chemistry package (Schmidt et al., 1993). Geometry optimizations used symmetry constraints appropriate to each molecule, and atomic positions in each molecule were optimized until the residual forces on each atom were less than  $10^{-5}$  hartree/bohr ( $\approx 8.24 \times 10^{-13}$  newtons). Vibrational frequencies were calculated at the optimized geometries.

It is well known (Pople et al., 1993; Scott and Radom, 1996; Wong, 1996) that ab initio force fields tend to make systematic errors in predicting vibrational frequencies. At the HF/6-31G(d) level, frequencies are typically overestimated by about 12%, with both high- and low-frequency vibrations off by roughly the same scale factor (Scott and Radom, 1996). In cases where the ab initio molecular structure is close to the observed structure (angles within  $1$  to  $2^\circ$ , bond lengths within  $\sim 0.02$  Å), and where calculated vibrational frequencies are proportional to the observed frequencies, the ratios of frequencies of isotopic molecules should be accurately predicted. However, we re-labeled the structural criteria slightly for  $\text{CCl}_3\text{F}$  and the ethylene-family molecules, where the calculated C-F and C=C bond lengths were off by 0.03 to 0.04 Å. The accuracy of the ab initio force-field calculations can be seen in Table 1, which compares observed, ab initio, and empirical force-field estimates of  $^{35}\text{Cl}$ - $^{37}\text{Cl}$  frequency shifts in a variety of molecules (including some where the ab initio model gives a poor fit to the observed structure). The HF/6-31G(d) models accurately predict the frequency shifts in isotopically substituted molecules, typically reproducing observed  $^{37}\nu/^{35}\nu$  ratios to within  $\sim 0.0005$ . As many as eighteen of the 26 ratios are reproduced within 0.0002 (depending on which experimental references are chosen), and the mean deviation is 0.0002. This level of accuracy corresponds to a difference of  $\sim 0.2$   $\text{cm}^{-1}$  in the isotopic shift of a  $500\text{-cm}^{-1}$  vibration, and it is often difficult to distinguish errors in the model force field from uncertainties in the measured shifts. Higher level ab initio calculations (B3LYP/6-31G(d), B3LYP/cc-pVTZ, MP2/cc-pVTZ) for  $\text{CCl}_4$ ,  $\text{CCl}_3\text{F}$ ,  $\text{C}_2\text{Cl}_4$ ,  $\text{ClNO}_2$ , and  $\text{ClO}_2$  predict  $^{35}\text{Cl}$ - $^{37}\text{Cl}$  frequency ratios within  $\sim 0.0004$  of HF/6-31G(d) models and observations, suggesting that our results are not very sensitive to the choice of ab initio method. Frequency ratios for  $\text{ClONO}_2$  are quite sensitive to the choice of ab initio method, however, and HF/6-31G(d) predicted shifts are not in good agreement with observations. Observed spectra of isotopically substituted species are complete for a few interesting molecules ( $[\text{ClO}_4]^-$ ,  $\text{CCl}_4$ ,  $\text{CH}_2\text{Cl}_2$  and  $\text{OCIO}$ ), and for these it will be possible to directly compare empirical- and ab initio-based fractionation models. For chlorine monoxide ( $\text{Cl}_2\text{O}$ ) and chlorine nitrate ( $\text{ClONO}_2$ ), ab initio modeling at the HF/6-31G(d) level gives grossly erroneous vibrational frequencies (off by  $>30\%$ ) and/or structures (one or more bond lengths off by more than 0.05 Å). For these molecules, we use both measured shifts and the shifts calculated with published empirical or high-level ab initio force fields, and/or shifts calculated with the Redlich-Teller product rule

Table 1. Comparison between observed, ab initio (HF/6-31G(d)), and empirical force-field-derived shifts in vibrational frequencies ( $^{37}\nu/^{35}\nu$ ). The symmetry of each vibrational mode is indicated in parentheses.

Species	Vibrational Mode	Frequency with $^{35}\text{Cl}$ ( $\text{cm}^{-1}$ )		No. of $^{37}\text{Cl}$ 's in substituted molecule	Mode symm. in substituted molecule	Frequency ratio ( $^{37}\nu/^{35}\nu$ )		
		Expt.	HF/6-31G(d)			Observed	Emp. FF	HF/6-31G(d)
$\text{SiCl}_4$	$\nu_3$ ( $F_2$ )	616.5	650.20	4	$F_2$	0.9908	0.9907	0.9910
$\text{CCl}_3\text{F}$	$\nu_1$ ( $A_1$ )	1081.28	1269.49	1	$A'$	0.9995	—	1.0000
	$\nu_2$ ( $A_1$ )	538.16	583.95	1	$A'$	0.9952 <sup>a</sup> , 0.9955 <sup>b</sup>	—	0.9951
$\text{CCl}_4$	$\nu_3$ ( $A_1$ )	351.41	385.25	1	$A'$	0.9938	—	0.9938
	$\nu_5$ ( $E$ )	838.5	966.51	1	$A'$	0.9984	—	0.9984
	$\nu_4$ ( $F_2$ )	313.6	348.25	1	$E$	0.9962	0.9962	0.9962
	$\nu_4$ ( $F_2$ )	313.6	348.25	1	$A_1$	0.9879	0.9879	0.9880
	$\nu_3$ ( $F_2$ )	779.01	902.40	1	$E$	0.9977	—	0.9976
$\text{CHCl}_3$	$\nu_3$ ( $F_2$ )	779.01	902.40	1	$A_1$	0.9997	—	0.9999
	$\nu_2$ ( $A_1$ )	675.5	730.74	3	$A_1$	0.9930	0.9926	0.9929
	$\nu_3$ ( $A_1$ )	366.8	403.47	3	$A_1$	0.9771	0.9770	0.9766
$\text{CH}_2\text{Cl}_2$	$\nu_5$ ( $E$ )	774.25	874.49	3	$E$	0.9952	0.9949	0.9950
	$\nu_3$ ( $A_1$ )	712.9	774.44	1	$A'$	0.9961 <sup>c</sup> , 0.9959 <sup>d</sup>	0.9954 <sup>c</sup>	0.9959
	$\nu_4$ ( $A_1$ )	281.5	311.82	1	$A'$	0.9879 <sup>c</sup>	—	0.9881
$\text{CH}_3\text{Cl}$	$\nu_9$ ( $B_2$ )	759.82	842.64	1	$A'$	0.9973 <sup>c</sup> , 0.9971 <sup>d</sup>	0.9971 <sup>c</sup>	0.9970
	$\nu_3$ ( $A_1$ )	732.84	782.60	1	$A_1$	0.9920	0.9918	0.9919
$\text{C}_2\text{Cl}_4$	$\nu_6$ ( $E$ )	1018.07	1138.36	1	$E$	0.99962	0.99961	0.99961
	$\nu_9$ ( $B_{2u}$ )	908	999.67	4	$B_{2u}$	0.9948	—	0.9947
$[\text{ClO}_4]^-$	$\nu_9$ ( $B_{3u}$ )	777	850.31	1	$A'$	0.9977	—	0.9982
	$\nu_3$ ( $F_2$ )	1101.5	1188.09	1	$F_2$	0.9867 <sup>f</sup> , 0.9879 <sup>g</sup>	0.9880 <sup>g</sup>	0.9874
$\text{ClNO}_2^{\text{h}}$	$\nu_4$ ( $F_2$ )	624	668.08	1	$F_2$	0.9952 <sup>f</sup>	0.9944 <sup>g</sup>	0.9949
	$\nu_2$ ( $A_1$ )	792.76	934.26	1	$A_1$	0.9994	—	0.9997
	$\nu_3$ ( $A_1$ )	370.15	519.20	1	$A_1$	0.9848	—	0.9848
$\text{Cl}_2\text{O}^{\text{i}}$	$\nu_1$ ( $A_1$ )	641.97	756.66	1	$A'$	0.9954	—	0.99512
$\text{OCIO}$	$\nu_1$ ( $A_1$ )	945.59	1067.94	1	$A_1$	0.9937	0.9937	0.9939
	$\nu_2$ ( $A_1$ )	447.70	507.65	1	$A_1$	0.9936	0.9936	0.9931

References:  $\text{SiCl}_4$  (Mohan and Müller, 1972);  $\text{CCl}_3\text{F}$  <sup>a</sup> (Snels et al., 2001), <sup>b</sup> (King, 1968);  $\text{CCl}_4$  (Jones et al., 1984);  $\text{CHCl}_3$  (Clark et al., 1976; Schmidt and Müller, 1974);  $\text{CH}_2\text{Cl}_2$  <sup>c</sup> (King, 1968), <sup>d</sup> (Duncan et al., 1987), <sup>e</sup> (Escribano et al., 1979);  $\text{CH}_3\text{Cl}$  (Black and Law, 2001);  $\text{C}_2\text{Cl}_4$  (Schnockel and Becher, 1975);  $[\text{ClO}_4]^-$  <sup>f</sup> (Chabanel et al., 1996), <sup>g</sup> (Decius and Murhammer, 1980);  $\text{ClNO}_2$  (Duxbury and Mcpheat, 1995; Orphal et al., 1998);  $\text{Cl}_2\text{O}$  (XU et al., 1996);  $\text{OCIO}$  (Müller et al., 1997b; Müller and Willner, 1993). <sup>h</sup> Ab initio model suspect because it predicts erroneous structures and frequencies. <sup>i</sup> Ab initio model suspect because it grossly overestimates the  $\nu_3$  ( $B_2$ ) frequency (calculated  $906 \text{ cm}^{-1}$ , observed  $687 \text{ cm}^{-1}$ )

(Nakamoto, 1997). In the remaining cases, shifts are determined by multiplying the ratios of frequencies in substituted and unsubstituted molecules calculated at the HF/6-31G(d) level by the observed frequencies for the  $^{35}\text{Cl}$ -end-member compositions.

Each calculated reduced partition function ratio is calculated for an exchange reaction placing a single  $^{37}\text{Cl}$  atom into a  $^{35}\text{Cl}$ -end-member molecule. In nature, this is the most common exchange reaction for molecules containing one to four chlorine atoms, given the terrestrial abundance of  $^{37}\text{Cl}$  and  $^{35}\text{Cl}$ . Calculated fractionations are insensitive to the choice of a particular exchange reaction, however, as a result of the nearly ideal mixing of chlorine isotopes in the molecules studied. Test calculations on  $\text{Cl}_2$ ,  $\text{CCl}_4$ ,  $\text{CHCl}_3$ ,  $\text{CH}_2\text{Cl}_2$ ,  $\text{CCl}_3\text{F}$  and  $\text{C}_2\text{Cl}_4$  suggest that the reduced partition function ratios calculated for the first  $^{37}\text{Cl}$  substitution are within  $\sim 0.1\%$  of all other possible single-atom exchange reactions at temperatures above 150 K, and within  $\sim 0.04\%$  above 273 K. This contrasts with other stable isotope systems, especially the hydrogen-deuterium system, where partition function ratios can change by tens or even hundreds of per mil for progressive single-atom exchange reactions (Richet et al., 1977). For chlorine, the differences are so small relative to other sources of theoretical error and measurement uncertainties that it is not presently necessary to distinguish between the different  $^{37}\text{Cl}$ -bearing forms of multiply chlorinated molecules with identical chlorine sites. The calculated reduced partition function ratios should accurately predict "bulk"  $^{37}\text{Cl}/^{35}\text{Cl}$  fractionations regardless of the  $^{37}\text{Cl}/^{35}\text{Cl}$  ratio of the system being studied.

The nearly ideal mixing of Cl-isotopes also suggests that if it were necessary to use a low-quality ab initio model to predict unknown

vibrational frequencies for a molecule, complete substitution of  $^{37}\text{Cl}$  for  $^{35}\text{Cl}$  might help mitigate modeling errors, because the full symmetry of the molecule would then be preserved. Vibrational frequencies and calculated shifts for  $^{37}\text{Cl}$ -substituted molecules are listed in Table 2.

### 2.3. Modeling Crystals

Unlike molecules, the vibrational spectra of most solids cannot be adequately measured by means of standard infrared and Raman spectroscopy. The technique of choice, inelastic neutron scattering, has only been rigorously applied to a handful of minerals. Luckily, several important chlorides have been studied this way. These include halite ( $\text{NaCl}$ ) (Raunio et al., 1969; Schmunk and Winder, 1970; Nilsson, 1979), sylvite ( $\text{KCl}$ ) (Raunio and Almquist, 1969),  $\text{RbCl}$  (Raunio and Rolandson, 1970b),  $\text{MnCl}_2$  (Escribe et al., 1980), and  $\text{FeCl}_2$  (Yelon et al., 1974). Phonon spectra of isotopically substituted chlorides have not been measured, nor have those of chlorine-bearing silicates, such as amphiboles, micas, and clays.

For the crystals with measured phonon spectra, it is necessary to create a lattice-dynamical model to predict unknown frequencies. Many such models have been proposed (i.e., Raunio and Rolandson 1970a). Long-range Coulomb forces and short-range bond forces are typically treated separately in these models, and the best of them (called shell models) take account of the mechanical and electrical polarizability of ions in the lattice. Models are typically constrained by using measured phonon spectra and additional information from elastic properties and/or dielectric constants.

Table 2. Vibrational frequencies of chlorine-bearing molecules and complexes. Only frequencies that are sensitive to  $^{37}\text{Cl}$ -substitution are listed. For each molecule, the ratio of the vibrational frequencies of  $^{37}\text{Cl}$ -substituted (one  $^{37}\text{Cl}$  per molecule) and  $^{35}\text{Cl}$ -end-member species were calculated using an ab initio (HF/6-31G(d)) model. The symmetry and degeneracy of each vibrational mode in the  $^{35}\text{Cl}$ -end-member molecule is indicated in parentheses. Isotopic substitution lowers the symmetry of some molecules, splitting degenerate vibrational modes into two or more distinct modes with different frequencies.

Species	Vibrational mode	Frequency with $^{35}\text{Cl}$ ( $\text{cm}^{-1}$ )	Frequency ratio ( $^{37}\nu/^{35}\nu$ ) HF/6-31G(d)	Degeneracy of mode in $^{37}\text{Cl}$ -bearing molecule
HCl	—	2990.92	0.99924 <sup>a</sup>	1
Cl <sub>2</sub>	—	559.7	0.98640 <sup>a</sup>	1
CCl <sub>3</sub> F	$\nu_1$ (A <sub>1</sub> , 1)	1081.28	0.99999	1
	$\nu_2$ (A <sub>1</sub> , 1)	538.16	0.99514	1
	$\nu_3$ (A <sub>1</sub> , 1)	351.41	0.99377	1
	$\nu_4$ (E, 2)	849.53	0.99993	1
			0.99838	1
	$\nu_5$ (E, 2)	399.2	0.99931	1
			0.99078	1
CCl <sub>4</sub>	$\nu_1$ (A <sub>1</sub> , 1)	460.2	0.99332	1
	$\nu_2$ (E, 2)	218.8	0.99310	2
	$\nu_3$ (F <sub>2</sub> , 3)	779.01	0.99992	2
			0.99756	1
	$\nu_4$ (F <sub>2</sub> , 3)	313.6	0.99621	2
			0.98797	1
			0.98797	1
CHCl <sub>3</sub>	$\nu_1$ (A <sub>1</sub> , 1)	3033.1	1.00000	1
	$\nu_2$ (A <sub>1</sub> , 1)	675.5	0.99758	1
	$\nu_3$ (A <sub>1</sub> , 1)	366.8	0.99242	1
	$\nu_4$ (E, 2)	1219.7	0.99999	1
			0.99986	1
	$\nu_5$ (E, 2)	773.7	0.99995	1
			0.99674	1
CH <sub>2</sub> Cl <sub>2</sub>	$\nu_1$ (A <sub>1</sub> , 1)	3122.6	1.00000	1
	$\nu_2$ (A <sub>1</sub> , 1)	1464.6	0.99999	1
	$\nu_3$ (A <sub>1</sub> , 1)	723.8	0.99588	1
	$\nu_4$ (A <sub>1</sub> , 1)	284.3	0.98806	1
	$\nu_5$ (A <sub>2</sub> , 1)	1176.5	0.99986	1
	$\nu_6$ (B <sub>1</sub> , 1)	3182.3	1.00000	1
	$\nu_7$ (B <sub>1</sub> , 1)	917.0	0.99968	1
	$\nu_8$ (B <sub>2</sub> , 1)	1294.8	0.99990	1
	$\nu_9$ (B <sub>2</sub> , 1)	771.4	0.99703	1
			0.99703	1
CH <sub>3</sub> Cl	$\nu_1$ (A <sub>1</sub> , 1)	3088.4	1.00000	1
	$\nu_2$ (A <sub>1</sub> , 1)	1396.3	0.99991	1
	$\nu_3$ (A <sub>1</sub> , 1)	751.2	0.99194	1
	$\nu_4$ (E, 2)	3183.3	1.00000	2
	$\nu_5$ (E, 2)	1496.2	0.99999	2
	$\nu_6$ (E, 2)	1036.8	0.99961	2
C <sub>2</sub> Cl <sub>4</sub>	$\nu_1$ (A <sub>g</sub> , 1)	1571	0.99997	1
	$\nu_2$ (A <sub>g</sub> , 1)	447	0.99336	1
	$\nu_3$ (A <sub>g</sub> , 1)	235	0.99323	1
	$\nu_4$ (A <sub>u</sub> , 1)	110	0.99319	1
	$\nu_5$ (B <sub>1g</sub> , 1)	1000	0.99954	1
	$\nu_6$ (B <sub>1g</sub> , 1)	347	0.99348	1
	$\nu_7$ (B <sub>1u</sub> , 1)	288	0.99901	1
	$\nu_8$ (B <sub>2g</sub> , 1)	512	0.99980	1
	$\nu_9$ (B <sub>2u</sub> , 1)	908	0.99869	1
	$\nu_{10}$ (B <sub>2u</sub> , 1)	176	0.99329	1
	$\nu_{11}$ (B <sub>3u</sub> , 1)	777	0.99821	1
	$\nu_{12}$ (B <sub>3u</sub> , 1)	310	0.99379	1
C <sub>2</sub> HCl <sub>3</sub>	$\nu_1$ (A', 1)	3082	1.00000/1.00000/1.00000 <sup>b</sup>	1
	$\nu_2$ (A', 1)	1586	0.99998/0.99996/0.99997 <sup>b</sup>	1
	$\nu_3$ (A', 1)	1247	1.00000/0.99995/0.99993 <sup>b</sup>	1
	$\nu_4$ (A', 1)	931	0.99880/0.99893/0.99967 <sup>b</sup>	1
	$\nu_5$ (A', 1)	780	0.99830/0.99996/0.99512 <sup>b</sup>	1
	$\nu_6$ (A', 1)	630	0.99891/0.99129/0.99983 <sup>b</sup>	1
	$\nu_7$ (A', 1)	384	0.98491/0.99834/0.99194 <sup>b</sup>	1
	$\nu_8$ (A', 1)	277	0.99053/0.99013/0.99506 <sup>b</sup>	1

(continued)

Table 2. (Continued)

Species	Vibrational mode	Frequency with $^{35}\text{Cl}$ ( $\text{cm}^{-1}$ )	Frequency ratio ( $^{37}\nu/^{35}\nu$ ) HF/6-31 G(d)	Degeneracy of mode in $^{37}\text{Cl}$ -bearing molecule
ClNO <sub>2</sub>	$\nu_9$ (A', 1)	178	0.99825/0.98698/98941 <sup>b</sup>	1
	$\nu_{10}$ (A'', 1)	840	0.99997/0.99999/0.99996 <sup>b</sup>	1
	$\nu_{11}$ (A'', 1)	451	0.99974/0.99905/0.99994 <sup>b</sup>	1
	$\nu_{12}$ (A'', 1)	215	0.99670/0.99991/0.99596 <sup>b</sup>	1
	$\nu_1$ (A <sub>1</sub> , 1)	1267.99	0.99999	1
	$\nu_2$ (A <sub>1</sub> , 1)	792.76	0.99971	1
	$\nu_3$ (A <sub>1</sub> , 1)	370.15	0.98482	1
	$\nu_4$ (B <sub>1</sub> , 1)	652.3	0.99959	1
	$\nu_5$ (B <sub>2</sub> , 1)	1683.89	1.00000	1
	$\nu_6$ (B <sub>2</sub> , 1)	408.1	0.99532	1
HOCl	$\nu_1$ (A', 1)	3794.1	1.00000	1
	$\nu_2$ (A', 1)	1271.6	0.99966	1
	$\nu_3$ (A', 1)	742.5	0.99125	1
Cl <sub>2</sub> O	$\nu_1$ (A <sub>1</sub> , 1)	641.97	0.99539 <sup>c</sup>	1
	$\nu_2$ (A <sub>1</sub> , 1)	300	0.98812 <sup>c</sup>	1
	$\nu_3$ (B <sub>2</sub> , 1)	686.59	0.99692 <sup>c</sup>	1
ClONO <sub>2</sub>	$\nu_1$ (A', 1)	1736.9	1.00000/0.999994 <sup>d</sup>	1
	$\nu_2$ (A', 1)	1292.7	1.00000/0.999992 <sup>d</sup>	1
	$\nu_3$ (A', 1)	809.4	0.99778/0.99792 <sup>d</sup>	1
	$\nu_4$ (A', 1)	780.2	0.99846/0.99826 <sup>d</sup>	1
	$\nu_5$ (A', 1)	563.1	0.99645/0.99690 <sup>d</sup>	1
	$\nu_6$ (A', 1)	434.0	0.99470/0.99371 <sup>d</sup>	1
	$\nu_7$ (A', 1)	273.3	0.98903/0.98956 <sup>d</sup>	1
	$\nu_8$ (A'', 1)	711.0	1.00000/0.99999 <sup>d</sup>	1
	$\nu_9$ (A'', 1)	121.9	0.99672/0.99643 <sup>d</sup>	1
ClO	—	853.72	0.99149 <sup>a</sup>	1
OCIO	$\nu_1$ (A <sub>1</sub> , 1)	945.59	0.99389	1
	$\nu_2$ (A <sub>1</sub> , 1)	447.70	0.99309	1
	$\nu_3$ (B <sub>2</sub> , 1)	1110.11	0.98916	1
[ClO <sub>4</sub> ] <sup>-</sup>	$\nu_3$ (F <sub>2</sub> , 3)	1115 <sup>c</sup>	0.98737	3
	$\nu_4$ (F <sub>2</sub> , 3)	630 <sup>c</sup>	0.99494	3

References: HCl (Parekunnel et al., 1999); Cl<sub>2</sub> (Clyne and Coxon, 1970); CCl<sub>3</sub>F, (Snels et al., 2001); CCl<sub>4</sub>, (Jones et al., 1984); CHCl<sub>3</sub>, (Clark et al., 1976; Schmidt and Müller, 1974); CH<sub>2</sub>Cl<sub>2</sub> (Duncan et al., 1987), (Escribano et al., 1979); CH<sub>3</sub>Cl, (Black and Law, 2001); C<sub>2</sub>Cl<sub>4</sub> (Castro and Anaconda, 1994); C<sub>2</sub>HCl<sub>3</sub>, (Schradler and Meier, 1974) as tabulated in (Kisiel and Pszczółkowski, 1996); ClNO<sub>2</sub>, (Duxbury and Mcpheat, 1995; Orphal et al., 1997); HOCl, (Abel et al., 1995); Cl<sub>2</sub>O, (Xu et al., 1996) for  $\nu_1$  and  $\nu_3$ , (Rochekind and Pimentel, 1965) for  $\nu_2$ ; ClONO<sub>2</sub>, (Orphal et al., 1997); ClO, (Burkholder et al., 1987); OCIO, (Müller et al., 1997b; Müller and Willner, 1993); [ClO<sub>4</sub>]<sup>-</sup>, (Chabanel et al., 1996) aqueous solution average.

<sup>a</sup> Frequency ratios calculated from atomic and isotopic masses.

<sup>b</sup> Frequency ratios are listed for C<sub>2</sub>HCl<sub>3</sub> molecules substituted at each of the three distinct Cl positions. The order in which the ratios are reported follows the labeling convention of Kisiel and Pszczółkowski (1996). The second ratio listed corresponds to a molecule with  $^{37}\text{Cl}$  at the position farthest from H, the 3<sup>rd</sup> ratio corresponds to a molecule with  $^{37}\text{Cl}$  at the position nearest H.

<sup>c</sup> These frequency ratios are taken from published spectra (Xu et al., 1996) and (for  $\nu_2$ ) the Redlich-Teller product rule, because HF/6-31G(d) ab initio model failed to give accurate vibrational frequencies for  $^{35}\text{Cl}_2\text{O}$ .

<sup>d</sup> Frequency ratios are taken from force-field calculation of Orphal et al. (1997) (on left) and Müller et al. (1997a) (on right), because HF/6-31G(d) ab initio model predicts an erroneous structure for ClONO<sub>2</sub>.

<sup>e</sup> Frequencies measured in aqueous solution.

FeCl<sub>2</sub> and MnCl<sub>2</sub> are important because they are the best available analogues for chlorine in silicates (Fig. 1). Chlorine is incorporated into the hydroxyl site in both amphiboles and biotite (Volfinger et al., 1985), and in both mineral types, the hydroxyl site is coordinated by three M<sup>2+</sup> cations that are themselves in six-fold coordination. Structural refinements and compositional evidence suggest that Cl<sup>-</sup> is strongly associated with Fe<sup>2+</sup> in these minerals (Volfinger et al., 1985; Makino and Tomita, 1993; Oberti et al., 1993), with a mean M<sup>2+</sup>-Cl<sup>-</sup> nearest-neighbor distance of ~2.46 Å. Chlorine in FeCl<sub>2</sub> has a local coordination environment (Vettier and Yelon, 1975) that is very similar to an amphibole or mica with Fe<sup>2+</sup>-Cl<sup>-</sup> clustering (Makino and Tomita, 1993; Oberti et al., 1993). Each chlorine atom in FeCl<sub>2</sub> is bonded to three Fe<sup>2+</sup> ions, with an Fe-Cl bond distance of ~2.50 Å. Thus, FeCl<sub>2</sub> may be a reasonable analogue for determining the chlorine-isotope fractionation behavior of silicates. MnCl<sub>2</sub> has the same basic structure and is much better studied spectroscopically, so it can help to confirm the FeCl<sub>2</sub> result. The best lattice-dynamics models available for both FeCl<sub>2</sub> and MnCl<sub>2</sub> are shell models similar to the ones developed for the

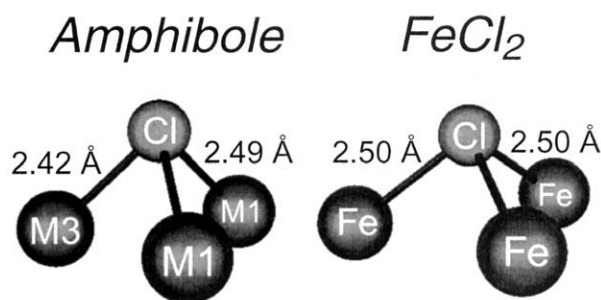


Fig. 1. Comparison of nearest-neighbor structures around chlorine in amphibole and FeCl<sub>2</sub>. In both structures, Cl<sup>-</sup> is bonded to three divalent cations, with average bond lengths of ~2.46 Å in Cl-rich amphibole and 2.50 Å in FeCl<sub>2</sub>. The pictured amphibole structure is from Makino and Tomita (1993), determined from a Cl-rich hastingsite. The FeCl<sub>2</sub> structure is from Vettier and Yelon (1975).

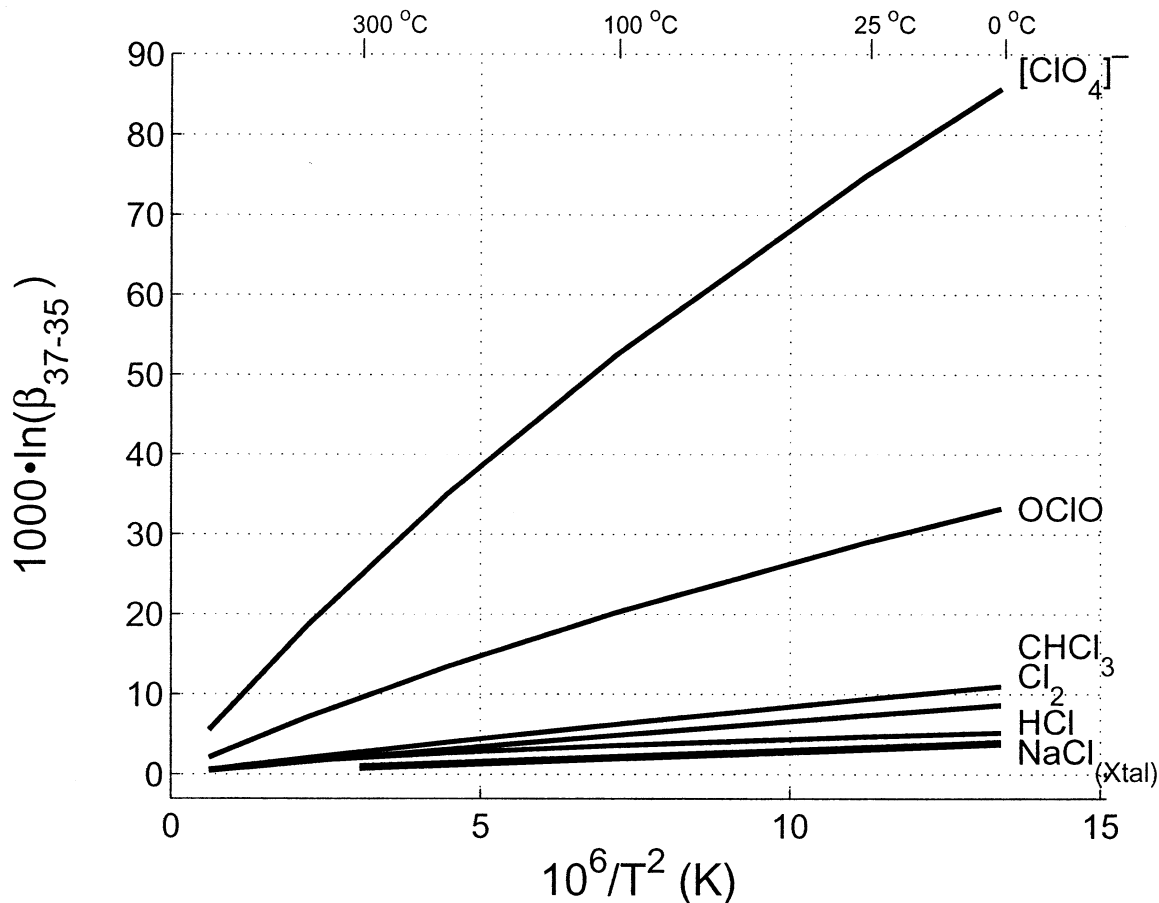


Fig. 2. Plot of calculated reduced partition function ratios for  $^{37}\text{Cl}$ - $^{35}\text{Cl}$  exchange [ $1000 \cdot \ln(\beta_{37-35})$ ] vs.  $10^6/T^2$  above 273 K for several substances studied (Tables 3 and 4).

alkali-halides (Benedek and Frey, 1980). In the present study, these models were used to calculate reduced partition function ratios.

In reproducing published lattice-dynamics models, it was typically necessary to convert force-field parameters from their original form into a form that available lattice-dynamics software could understand. We found small differences between the frequencies we calculated and those reported by the original authors. For the most part the discrepancies are very small, on the order of 1 to 2%, and it is likely that these differences arise from the conversion process, or possibly from slight differences in the physical constants and computational techniques used. We found it helpful to reoptimize these models to the measured frequencies for each substance. Most of the models were found to rapidly converge with only modest changes in the converted parameters; and residual errors for the reoptimized models are similar to the errors reported for the original models. Differences in calculated reduced partition function ratios between reoptimized and unreoptimized models are modest, 0.3% or less at 273 K. Furthermore, reoptimization substantially reduced the scatter between different models for a given crystal. Three of the NaCl models developed in (Raunio and Rolandson, 1970a) are exceptions. There are large discrepancies between the observed and calculated frequencies among these three models, and it even appears that Na-Na and Cl-Cl interaction terms were switched for two of these models. After reoptimization, however, the models predict reduced partition function ratios that are very similar to those based on the other lattice dynamics models for NaCl, even those that were reoptimized to a different set of measured frequencies. The models were all optimized assuming that the atomic mass of chlorine is 35.453 amu.

All lattice-dynamics calculations are made by GULP, the General Utility Lattice Program (Gale, 1997). Reduced partition function ratios

are calculated from the Helmholtz free energies of  $^{35}\text{Cl}$ - and  $^{37}\text{Cl}$ -end-member compositions by eqn. 15 of Kieffer (1982). In order to determine the Helmholtz free energy of each model crystal it is necessary to integrate phonon frequencies across the entire volume of the Brillouin zone, representing all possible phonon wave vectors in that crystal. This is done numerically by sampling discrete, symmetrically distinct wave vectors in the Brillouin zone. To make sure that the numerical integration was not affecting the calculated properties, the number of sampling points was varied from 1 to ~1000. It was found that the calculated change in the Helmholtz free energy attributable to isotope substitution converged very rapidly as the number of sampling points increased, varying by no more than  $2 \cdot 10^{-3}$  J/mol for runs with 20 or more sampling points. The resulting error in a calculated reduced partition function ratio is ~0.001% at 298 K, indicating that numerical integration is not a significant source of uncertainty. Elcombe and Hulston (1975) report a similar rate of convergence in calculating sulfur isotope fractionations between sphalerite (ZnS) and galena (PbS). For the present study, roughly 150 wave vectors were sampled in calculating each reduced partition function ratio.

### 3. RESULTS

#### 3.1. Calculated Fractionations

Calculated reduced partition function ratios for  $^{37}\text{Cl}$ - $^{35}\text{Cl}$  exchange from 273 K (0°C) to at least 573 K (300°C) are shown in Figures 2 to 5 and Tables 3 and 4. Calculations for molecules cover an extended range of temperatures from 153 K

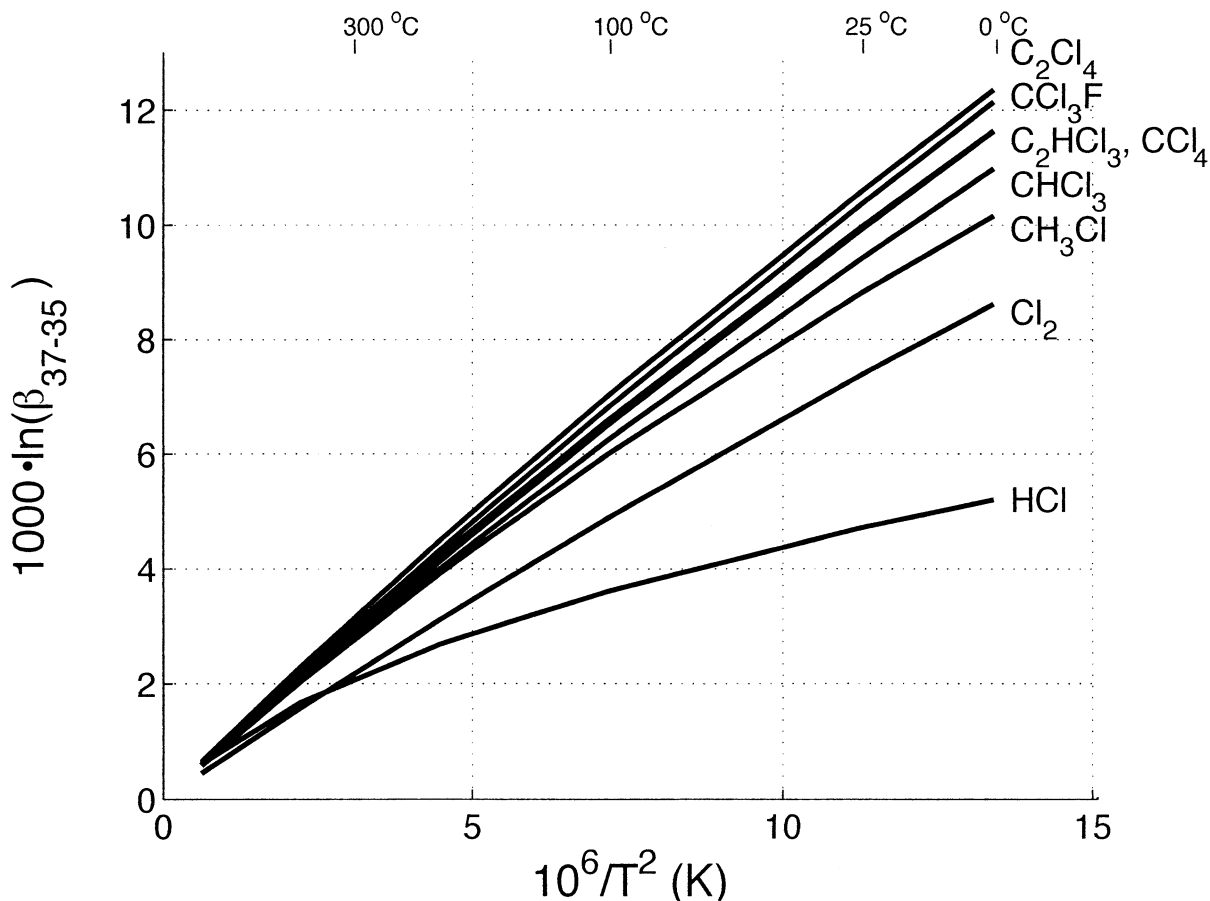


Fig. 3. Plot of calculated reduced partition function ratios for  $^{37}\text{Cl}$ - $^{35}\text{Cl}$  exchange [ $1000 \cdot \ln(\beta_{37-35})$ ] vs.  $10^6/T^2$  in small Cl-bearing organic molecules (Table 3).

( $-120^\circ\text{C}$ ) to 1273 K ( $1000^\circ\text{C}$ ). Most calculated reduced partition function ratios are approximately proportional to  $1/T^2$  ( $T$  in Kelvin) over the temperature range considered, especially at  $T > 273$  K. The reduced partition function ratio calculated for HCl behaves differently, however, because its vibrational frequency is so high. Calculated  $1000 \cdot \ln(\beta_{37-35})$  values at 298 K ( $25^\circ\text{C}$ ) range from  $\sim 2.3$  per mil for RbCl to 75 per mil for  $[\text{ClO}_4]^-$ , a range comparable to that observed in the sulfur isotope ( $^{34}\text{S}$ - $^{32}\text{S}$ ) system (Richet et al., 1977). The three Cl positions in trichloroethylene ( $\text{C}_2\text{HCl}_3$ ) are predicted to have different affinities for  $^{37}\text{Cl}$ . At equilibrium and 298 K, the Cl closest to the H-atom in this molecule will be  $\sim 1\%$  lighter than the Cl farthest from the H atom. The calculations assumed no internal rotation about the C=C double bond, which may not be accurate at higher temperatures.

Equilibrium  $^{37}\text{Cl}$ - $^{35}\text{Cl}$  fractionations for a few molecules (HCl,  $\text{Cl}_2$ ,  $\text{ClO}_2$ , and  $[\text{ClO}_4]^-$ ,  $\text{CCl}_4$ ,  $\text{ClNO}_2$ ) in the present study have previously been calculated by other authors (Urey, 1947; Kotaka and Kakihana, 1977; Richet et al., 1977; Hanschmann, 1984), and our results agree at least qualitatively with earlier work. For HCl,  $\text{Cl}_2$ , and  $\text{CCl}_4$  disagreement in  $1000 \cdot \ln(\beta_{37-35})$  between our work and previous studies is  $\leq 0.3\%$ ,  $\leq 0.1\%$ , and  $\leq 0.3\%$ , respectively, over the range from  $0^\circ\text{C}$  to  $1000^\circ\text{C}$ . For HCl and  $\text{Cl}_2$ , this good agreement is hardly surprising, because the vibrational spectra for these two molecules

were accurately measured many decades ago. In addition, vibrational frequencies for  $^{37}\text{Cl}$ -bearing diatomic molecules are easily calculated without any need for a force-field model, and there is good agreement between the calculated and observed frequencies. For  $\text{CCl}_4$ , Kotaka and Kakihana (1977) used an empirical force-field model to calculate frequencies for  $\text{C}^{37}\text{Cl}_4$ , and the similarity between their result and ours follows from the similarity between frequency shifts calculated with empirical and ab initio force-field models (Table 1). For  $\text{ClO}_2$  and the  $[\text{ClO}_4]^-$  anion, our calculated  $1000 \cdot \ln(\beta_{37-35})$  values are  $\sim 2.2\%$  and  $8\%$  lower, respectively, than the values reported by Urey (1947) at  $0^\circ\text{C}$ . The  $\nu_2$  vibrational frequency in  $\text{ClO}_2$  is now known to be much lower than was thought in 1947 ( $448 \text{ cm}^{-1}$  vs.  $529 \text{ cm}^{-1}$ ), and this difference is largely responsible for the change in calculated  $1000 \cdot \ln(\beta_{37-35}[\text{ClO}_2])$ . For  $[\text{ClO}_4]^-$ , vibrational frequencies of the  $[\text{ClO}_4]^-$  end-member used by Urey (1947) are very similar to the frequencies we used. The difference in the calculated reduced partition function ratios is attributable almost entirely to differences in the calculated frequencies for  $[\text{ClO}_4]^-$ . Urey's valence force-field model predicts a large shift ( $16.7 \text{ cm}^{-1}$ ,  $^{37}\nu^{35}\nu \approx 0.9849$ ) in the high-frequency  $\nu_3$  vibration upon substitution of  $^{37}\text{Cl}$ . Measured spectra show a smaller shift of 13 to  $15 \text{ cm}^{-1}$  (Chabanel et al., 1996; Decius and Murhammer, 1980), consistent with our calculated shift of  $14.1 \text{ cm}^{-1}$ . Present calculations for both

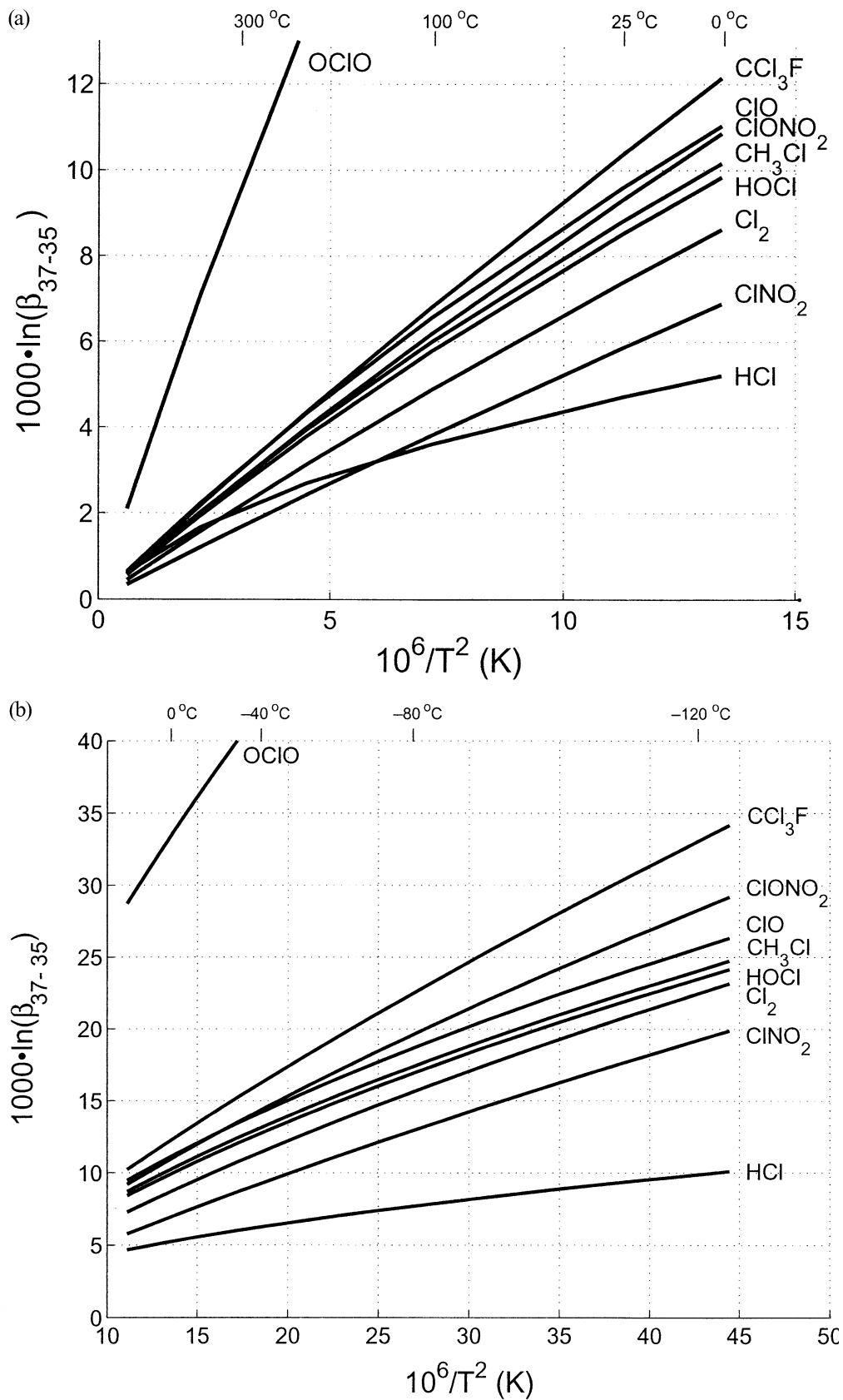


Fig. 4. Plot of calculated reduced partition function ratios  $^{37}\text{Cl}$ - $^{35}\text{Cl}$  exchange [ $1000 \cdot \ln(\beta_{37-35})$ ] vs.  $10^6/T^2$  in molecules of interest in atmospheric chemistry (Table 3). (a) Temperatures above 273 K. (b) Temperatures from 150 K to 273 K.



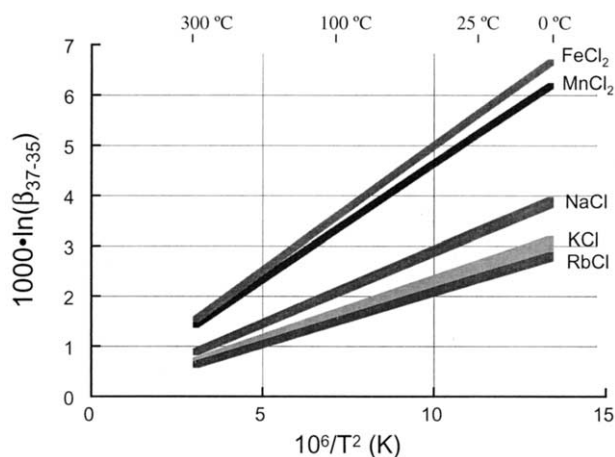


Fig. 5. Plot of calculated reduced partition function ratios  $^{37}\text{Cl}$ - $^{35}\text{Cl}$  exchange [ $1000 \cdot \ln(\beta_{37-35})$ ] vs.  $10^6/T^2$  in solid chlorides. The thicknesses of lines plotted for NaCl, KCl, and RbCl represent ranges calculated by means of different reoptimized lattice dynamics models (see text).

$\text{ClO}_2$  and  $[\text{ClO}_4]^-$ , therefore, are probably more accurate than those reported previously. The results of Hanschmann (1984) for HCl,  $\text{ClNO}_2$ ,  $\text{Cl}_2$ ,  $\text{ClO}_2$ , and  $[\text{ClO}_4]^-$  are much less concordant with our calculations and earlier models. Although there is a qualitative agreement between Hanschmann (1984), Urey (1947), and the present work in terms of relative ordering of high  $^{37}\text{Cl}/^{35}\text{Cl}$  and low  $^{37}\text{Cl}/^{35}\text{Cl}$  species, Hanschmann (1984) calculates much lower reduced partition function ratios for HCl,  $\text{ClO}_2$ , and  $[\text{ClO}_4]^-$  (by roughly 2%, 10% and >20% at 300 K, respectively), and higher reduced partition function ratios for  $\text{Cl}_2$  and  $\text{ClNO}_2$  (by  $\sim 1.5\%$  at 300 K). This may reflect the use of calculated frequencies for both  $^{35}\text{Cl}$ -bearing

and  $^{37}\text{Cl}$ -bearing forms of these molecules. Semi-empirical quantum-mechanical models similar to those used by Hanschmann (1984) often generate inaccurate vibrational frequencies (Scott and Radom, 1996), possibly causing the large disagreements in calculated isotopic fractionations.

### 3.2. Accuracy Estimates

Calculated reduced partition function ratios may be in error for several reasons: (1) uncertainty in the measured or (in the case of crystals) calculated vibrational frequencies for  $^{35}\text{Cl}$ -end-member substances; (2) errors in the frequency shifts calculated for  $^{37}\text{Cl}$  substitution; and (3) anharmonicity effects.

In general, the vibrational frequencies of  $^{35}\text{Cl}$  end-member molecular species are known to a high degree of accuracy. Except for  $[\text{ClO}_4]^-$ , the studied species are all neutral and amenable to spectroscopic measurement in the gas phase and/or in noble-gas matrices. The fundamental vibrational frequencies for these species are reliable to within one or at most a few  $\text{cm}^{-1}$ . Propagated errors in the reduced partition function ratios for measurement uncertainties of this size are quite small, as random shifts of  $2 \text{ cm}^{-1}$  change  $1000 \cdot \ln(\beta_{37-35})$  by less than 0.2‰ for all of the neutral molecules at temperatures above 273 K.

The perchlorate anion,  $[\text{ClO}_4]^-$ , does not lend itself to gas-phase measurements, and its geochemical relevance is as a solute species. The vibrational frequency of the  $\nu_3$  mode of  $[\text{ClO}_4]^-$  in solution varies over a range of  $\sim 25 \text{ cm}^{-1}$  depending on the type of solution, whereas the  $\nu_4$  mode varies over a range of  $\sim 10 \text{ cm}^{-1}$  (Chabanel et al., 1996). This suggests that  $1000 \cdot \ln(\beta_{37-35}[\text{ClO}_4]^-)$  could vary by several per mil, depending on the solution chemistry. Although that error is quite large relative to errors for gas-phase molecules, it is much smaller than the predicted fractionation between  $[\text{ClO}_4]^-$  and

Table 3. Calculated reduced partition function ratios [ $1000 \cdot \ln(\beta_{37-35})$ ] for  $^{37}\text{Cl}$ - $^{35}\text{Cl}$  exchange in molecules at various temperatures. Linear interpolation (with respect to  $1/T$ ,  $T$  in Kelvin, at temperatures below  $100^\circ\text{C}$  and  $1/T^2$  at higher temperatures) between the temperatures reported here will reproduce the curves shown in Figs. 2 to 4 to within 0.3‰ (0.1‰ excepting  $[\text{ClO}_4]^-$ ).

Molecule	$-120^\circ\text{C}$	$-100^\circ\text{C}$	$-80^\circ\text{C}$	$-40^\circ\text{C}$	$0^\circ\text{C}$	$25^\circ\text{C}$	$100^\circ\text{C}$	$200^\circ\text{C}$	$400^\circ\text{C}$	$1000^\circ\text{C}$
$\text{Cl}_2$	22.45	18.56	15.57	11.36	8.62	7.37	4.88	3.11	1.57	0.45
HCl	9.88	8.65	7.68	6.23	5.21	4.71	3.61	2.69	1.67	0.61
$\text{C}_2\text{Cl}_4$	32.83	26.91	22.46	16.30	12.35	10.56	7.01	4.49	2.28	0.65
$\text{C}_2\text{HCl}_3^a$	Cl-1: 31.08	25.47	21.23	15.39	11.64	9.95	6.59	4.21	2.14	0.61
	Cl-2: 31.96	26.35	22.08	16.13	12.26	10.50	6.99	4.49	2.28	0.65
	Cl-3: 28.60	23.58	19.78	14.47	11.02	9.45	6.31	4.06	2.07	0.59
	Mean: 30.55	25.13	21.03	15.33	11.64	9.97	6.63	4.25	2.16	0.62
$\text{CCl}_3\text{F}$	33.17	27.08	22.50	16.20	12.19	10.39	6.84	4.35	2.19	0.62
$\text{CCl}_4$	32.03	26.06	21.60	15.50	11.63	9.90	6.50	4.13	2.08	0.59
$\text{CHCl}_3$	28.93	23.78	19.88	14.47	10.98	9.40	6.24	4.00	2.03	0.58
$\text{CH}_2\text{Cl}_2$	26.32	21.90	18.51	13.70	10.53	9.06	6.10	3.95	2.02	0.58
$\text{CH}_3\text{Cl}$	24.05	20.29	17.34	13.06	10.16	8.80	6.00	3.92	2.03	0.59
$\text{ClNO}_2$	19.21	15.60	12.89	9.21	6.88	5.84	3.82	2.41	1.21	0.34
$\text{Cl}_2\text{O}$	23.18	19.12	16.03	11.70	8.88	7.60	5.04	3.23	1.64	0.47
HOCl	23.48	19.78	16.88	12.68	9.83	8.51	5.78	3.77	1.94	0.56
$\text{ClONO}_2$ #1	27.91	23.02	19.30	14.10	10.72	9.18	6.10	3.91	1.99	0.57
$\text{ClONO}_2$ #2	28.27	23.32	19.55	14.28	10.85	9.29	6.18	3.96	2.01	0.57
ClO	25.62	21.70	18.62	14.12	11.03	9.58	6.56	4.30	2.23	0.65
OCIO	74.66	63.54	54.80	42.01	33.20	29.01	20.20	13.46	7.10	2.09
$[\text{ClO}_4]^-$	190.32	162.41	140.40	108.06	85.68	74.99	52.44	34.06	18.58	5.49

<sup>a</sup> Beta factors were calculated for each of the three Cl positions in  $\text{C}_2\text{HCl}_3$ . Results are labeled according to the convention of Kisiel and Pszczółkowski (1996). Cl-2 corresponds to the Cl position farthest from H, and Cl-3 corresponds to the Cl closest to H.

Table 4. Calculated reduced partition function ratios [ $1000 \cdot \ln(\beta_{37-35})$ ] for  $^{37}\text{Cl}$ - $^{35}\text{Cl}$  exchange in NaCl (halite), KCl (sylvite), RbCl,  $\text{MnCl}_2$ , and  $\text{FeCl}_2$ . For the alkali halides, each tabulated result is the mean of several re-optimized lattice dynamics models. Numbers in parentheses show the number of models averaged and the standard deviation at each temperature. Linear interpolation (with respect to  $1/T^2$ ) between the temperatures reported here will reproduce the curves shown in Fig. 4 to within 0.1‰.

Crystal	0°C	25°C	100°C	300°C
NaCl (n = 4)	3.87 (0.060)	3.26 (0.050)	2.09 (0.032)	0.89 (0.014)
KCl (n = 6)	2.96 (0.070)	2.48 (0.059)	1.59 (0.038)	0.68 (0.016)
RbCl (n = 3)	2.78 (0.034)	2.34 (0.028)	1.50 (0.018)	0.64 (0.008)
$\text{FeCl}_2$	6.66	5.61	3.60	1.54
$\text{MnCl}_2$	6.20	5.22	3.35	1.43

References: NaCl – 3 models (Raunio and Rolandson, 1970a) were reoptimized to frequencies reported by Raunio et al. (1969); model II from Schmunk and Winder (1970) was not reoptimized because the measured frequencies are not tabulated. KCl – 3 models (Raunio and Rolandson, 1970a) were reoptimized to frequencies reported in Raunio and Almquist (1969); the Copley et al. (1969) models (II, V, and VI) were reoptimized to the (Copley et al., 1969) measured frequencies. RbCl – 3 models (Raunio and Rolandson, 1970a) were reoptimized to frequencies reported by Raunio and Rolandson (1970b).  $\text{FeCl}_2$  and  $\text{MnCl}_2$  – models (Benedek and Frey, 1980) were not reoptimized.

other substances. Vibrational frequencies for neutral molecules may also change when they are dissolved in a liquid, adsorbed, or are held at high pressure. In addition, rotational and translational degrees of freedom are often hindered when molecules dissolve or condense, creating new Cl-isotope sensitive vibrational modes. These solution effects could be much larger than 0.1‰. Preliminary experiments (Huang et al., 1999) suggest that small organic molecules in solution tend to concentrate  $^{37}\text{Cl}$  relative to the gas phase, with equilibrium vapor-liquid fractionations as large as 0.5‰ observed for trichloroethylene ( $\text{C}_2\text{HCl}_3$ ), and 0.1‰ for dichloromethane ( $\text{CH}_2\text{Cl}_2$ ) at room temperature.

For crystals, uncertainty in vibrational (phonon) frequencies of  $^{35}\text{Cl}$ -end-member compositions may be a significant source of error. It is time-consuming to measure vibrations with inelastic neutron scattering, and measurements are usually limited to wave-vectors along high-symmetry directions in the Brillouin zone. Thermodynamic properties, however, are largely determined by off-symmetry wave vectors, and lattice dynamics models can be used to make the necessary extrapolation. The reoptimized lattice dynamics models for NaCl, KCl, and RbCl reproduce measured high-symmetry frequencies within  $\sim 1$ – $2\%$ , but for KCl and RbCl we don't know how well the rest of the vibrational spectrum is predicted. For NaCl, a large number of off-symmetry vibrational frequencies have been measured (Nilsson, 1979), and it is possible to compare those frequencies with model predictions. Surprisingly, measured off-symmetry frequencies turn out to be very close to the calculated frequencies, typically within 1–2%, suggesting (at least for NaCl) that the reoptimized lattice dynamics models are fairly accurate. Note that a uniform 1% shift in vibrational frequencies for NaCl would change the calculated  $1000 \cdot \ln(\beta_{37-35}[\text{NaCl}])$  by  $\sim 0.08\%$  at 0°C, and at higher temperatures the size of this error is approximately proportional to  $1/T^2$ . For KCl and RbCl, equivalent measurement errors would propagate to somewhat smaller errors of  $\sim 0.06\%$  at 0°C.

Spectroscopic measurements on  $\text{FeCl}_2$  and  $\text{MnCl}_2$  are not as extensive as for the alkali halides, limiting the accuracy of calculated reduced partition function ratios for these substances. In addition, the lattice dynamics models do not match measured frequencies as well.  $\text{MnCl}_2$  is the better studied of the two, and frequencies calculated with the model of Benedek and Frey (1980) are generally within a few percent of measured

frequencies. However, frequencies are about 10% too high in one longitudinal optical (LO) branch of  $A_1$  symmetry, and  $>10\%$  too high in the longitudinal acoustic (LA) phonon branch in the  $\Gamma$ -K direction, and this could lead to errors as large as 0.7‰ in the predicted  $1000 \cdot \ln(\beta_{37-35})$  at 0°C.

For crystalline solids, and molecules containing more than two atoms, the largest sources of error in our calculations probably come from uncertainties in the predicted frequencies for  $^{37}\text{Cl}$ -bearing species. This problem is particularly acute for molecules in which two or more vibrations at moderate to low frequencies (0 to  $\sim 1000 \text{ cm}^{-1}$ ) have the same symmetry. Higher frequency vibrations are usually only slightly sensitive to Cl-isotope substitution and are therefore less important. A large data set is available for  $^{37}\text{Cl}$ -bearing molecular species that can be used to check the ab initio force-field models (Table 1). These comparisons suggest that ab initio modeling reproduces observed frequency shifts ( $^{37}\nu/^{35}\nu$ ) to within about 0.0005 in most cases, in agreement with our earlier findings utilizing empirical force fields (Schauble et al., 2001).

For  $[\text{ClO}_4]^-$ ,  $\text{CCl}_4$ ,  $\text{CH}_2\text{Cl}_2$  and  $\text{OCIO}$ , it is possible to use measured frequencies for  $^{37}\text{Cl}$ -bearing species to calculate  $1000 \cdot \ln(\beta_{37-35})$  and thus directly estimate the effects of force-field errors. Measured shifts for  $[\text{ClO}_4]^-$ ,  $\text{CCl}_4$ ,  $\text{CH}_2\text{Cl}_2$  and  $\text{OCIO}$  give results that differ by 3.07, 0.32, 0.28 and 0.13‰ at 25°C, respectively. If we perturb the calculated frequency shifts (for moderate-low frequency vibrations) for other molecules by a similar amount (0.0003 to 0.0005) in a way consistent with the Redlich-Teller product rule, the calculated values of  $1000 \cdot \ln(\beta_{37-35})$  change by about 0.1 to 0.7‰ (at 298 K). The sensitivity of the calculated values of  $1000 \cdot \ln(\beta_{37-35})$  to errors in calculated vibrational frequencies is greatest for higher frequency vibrations, particularly when vibrations of the same symmetry have very different frequencies (i.e.,  $\nu_3$  vs.  $\nu_4$  in  $\text{CCl}_4$ ). It is, unfortunately, not possible to give a quantitative estimate of errors in calculated frequencies for  $^{37}\text{Cl}$ -bearing crystals. However, the general agreement between several lattice-dynamics models (of varying complexity) for each crystalline chloride provides some assurance that the results are not grossly erroneous.

The calculations reported here assume that molecular and crystalline vibrations are harmonic, mostly out of necessity because vibrational anharmonicity has not been quantified for many of the substances of interest. Resulting errors are prob-

ably small for the molecules we studied, at least over the temperature range of interest, but they may be significant for the chloride crystals. We estimate that typical molecular anharmonicities of  $\sim 1\%$  will cause errors of 0.1 to 0.2‰ for most molecules. Larger errors of up to 0.5‰ and 2‰ may result for  $\text{ClO}_2$  and  $[\text{ClO}_4]^-$ , respectively. In compiling molecular vibrational frequencies, we have used a number of data that have been “corrected” for anharmonicity by measured overtone- and combination-band frequencies. Zero-point energies should be more accurately approximated with corrected frequencies than by using the raw, measured fundamental frequencies; therefore, we have used the corrected frequencies when they are available.

In crystals, and particularly in halides like NaCl, anharmonicity typically causes vibrational frequencies to decrease with increasing temperature. The frequencies used to constrain the lattice-dynamics calculations for crystals were, for the most part, measured at very low temperatures (77 to 120 K). Measurements made at  $\sim 300$  K in NaCl (Raunio et al., 1969; Schmunk and Winder, 1970), KCl (Tanaka and Hisano, 1989; Wakamura, 1993), and RbCl (Raunio and Rolandson, 1970b) suggest that vibrational frequencies are typically  $\sim 2$  to 5% lower at this temperature than at  $\sim 120$  K. As a consequence, the calculated values of  $1000 \cdot \ln(\beta_{37-35})$  for NaCl, KCl, and RbCl are probably  $\sim 0.1$  to 0.4‰ too high at room temperature. The estimated error of 0.1–0.4‰ may be reasonable over the entire temperature range of interest, because further reductions in vibrational frequencies at higher temperatures are counterbalanced by rapid decreases in absolute  $1000 \cdot \ln(\beta_{37-35})$  values. There do not appear to be any major differences in the temperature dependence of phonon frequencies in the different alkali halides, so the effect is expected to be approximately the same for all of them. The same types of errors probably affect calculations for  $\text{FeCl}_2$  and  $\text{MnCl}_2$ , but there is not enough information justify a quantitative error estimate.

Combining all three sources of error described above, it is possible to make a rough estimate of the total errors in calculated  $1000 \cdot \ln(\beta_{37-35})$  values. For  $[\text{ClO}_4]^-$ , the total error amounts to approximately  $\pm 5\%$  at 298 K. For the gas-phase molecules,  $\text{OClO}$ :  $\pm 1\%$ ,  $\text{HCl}$  and  $\text{Cl}_2$ :  $\pm 0.3\%$ , other molecules:  $\pm 0.5\%$  to  $0.8\%$ . In general, errors are largest for molecules that tend to concentrate  $^{37}\text{Cl}$ , and for molecules with three or more atoms. Because we cannot compare model and measured frequencies for  $^{37}\text{Cl}$ -bearing crystals, the combined error estimates for crystals should be considered lower bounds on the true errors. Uncertainties in model frequencies of  $^{35}\text{Cl}$ -dominated crystals and the lack of consideration of anharmonicity (T-dependence of vibrational frequencies) lead to errors of approximately  $+0.0\%$ – $-0.5\%$  for NaCl, KCl, and RbCl. Errors in model frequencies of  $\text{Fe}^{35}\text{Cl}_2$  and  $\text{Mn}^{35}\text{Cl}_2$  could cause errors as large as  $\pm 0.7\%$  at  $25^\circ\text{C}$ , anharmonic effects certainly increase this uncertainty. Errors are likely to be smaller when closely related species are compared (i.e., NaCl vs. RbCl) than they will be for chemically distinct species (i.e.,  $\text{ClONO}_2$  vs.  $\text{FeCl}_2$ ).

#### 4. DISCUSSION

##### 4.1. Factors Controlling Predicted Fractionations

Predicted reduced partition function ratios are determined from vibrational frequencies of Cl-bearing substances and by

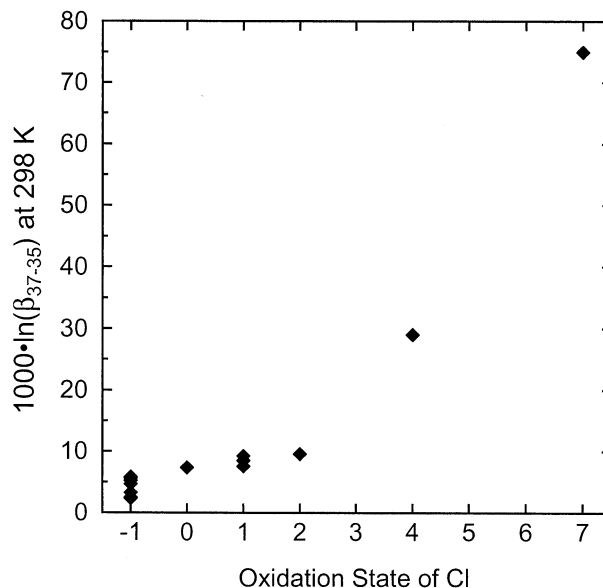


Fig. 6. Correlation between calculated reduced partition function ratios (at 298 K) and the oxidation state of chlorine in substances containing Cl-metal and Cl-O bonds. Chlorine-bearing organic species have been excluded from this plot.

the sensitivities of those vibrations to Cl-isotope substitution. Molecules and crystals with high-frequency, highly Cl-isotope sensitive vibrations will tend to concentrate  $^{37}\text{Cl}$ . The tremendous range in the masses of bonding partners for Cl, however, means that there is a poor correlation between the frequency of Cl-X stretching vibrations and calculated values of  $1000 \cdot \ln(\beta_{37-35})$ . A good correlation is found between  $1000 \cdot \ln(\beta_{37-35})$  and the oxidation state of chlorine (Fig. 6). Substances with oxidized chlorine ( $\text{Cl}^{1+}$ ,  $\text{Cl}^{2+}$ ,  $\text{Cl}^{7+}$ , etc.) will tend to have higher  $^{37}\text{Cl}/^{35}\text{Cl}$  ratios than crystals containing  $\text{Cl}^-$ . For molecules with C-Cl bonds, covalent bonding makes assigning an oxidation state less clear-cut. These substances are similar to typical  $\text{Cl}^0$  and  $\text{Cl}^{1+}$  molecules in their affinities for  $^{37}\text{Cl}$ . Furthermore, the chlorine-bearing organic molecules studied are all similar to one another, spanning a total range of  $\sim 1.8\%$  at room temperature. For metal chlorides, there is a strong effect exerted by the bond partner; crystals with  $\text{M}^{1+}$ -Cl bonds (i.e., NaCl, KCl, and RbCl) will tend to have low  $^{37}\text{Cl}/^{35}\text{Cl}$  ratios when in equilibrium with crystals having  $\text{M}^{2+}$ -Cl bonds ( $\text{FeCl}_2$ ,  $\text{MnCl}_2$ ). Previous modeling of aqueous  $[\text{M}^{4+}\text{Cl}_6]^{2-}$  complexes (Kotaka et al., 1978) suggests that they will also have higher  $^{37}\text{Cl}/^{35}\text{Cl}$  than coexisting  $\text{M}^{1+}\text{Cl}$  crystals. At low temperatures, HCl follows this trend, but here the tiny mass of the H atom is a more important factor than its oxidation state. At high temperatures, where bond stiffness is most important, HCl is similar to the chlorine-bearing organic molecules (with C-Cl bonds) in its affinity for  $^{37}\text{Cl}$ . A similar bond partner mass effect may control relative fractionations among the organic molecules, though here the relevant mass is the entire molecule, not just the nearest-neighbor atom. The heaviest molecules studied (i.e.,  $\text{C}_2\text{Cl}_4$ ,  $\text{CCl}_4$ ,  $\text{CCl}_3\text{F}$ ) are predicted to concentrate  $^{37}\text{Cl}$  relative to lighter, more H-rich molecules like  $\text{CH}_3\text{Cl}$ . C-Cl bonds are probably the least stiff bonds in a small organic molecule, so the C-atom and some of its other bond partners (even other Cls)

behave as a single quasicohesive mass during C-Cl stretching vibrations. The heavier the effective counter-mass, the greater the sensitivity of the Cl-C stretching vibrations to Cl-isotope substitution, leading to a greater affinity for  $^{37}\text{Cl}$ . A large counter-mass will also tend to reduce the Cl-C stretching frequency, which may explain the poor correlation between Cl-X stretch frequencies and  $1000 \cdot \ln(\beta_{37-35})$  among Cl-bearing organic molecules. This counter-mass effect may also control internal fractionation in trichloroethylene ( $\text{C}_2\text{HCl}_3$ ), with heavy Cl tending to be concentrated in the part of the molecule farthest from the light H atom. Among the alkali chlorides, we predict a progressive decrease in  $^{37}\text{Cl}/^{35}\text{Cl}$  ratios going from NaCl to KCl and RbCl, consistent with the larger ionic radii and consequently softer M-Cl bonds of  $\text{K}^+$  and  $\text{Rb}^+$  cations relative to  $\text{Na}^+$ .

#### 4.2. Comparison with Experimental Results and Natural Samples

The best way to evaluate the accuracy of predicted fractionations is to compare them with high-quality experimental measurements. Estimated errors for calculated fractionations are large relative to the typical precision of a Cl-isotope measurement, so even if our predictions are correct, significant refinement should be possible through careful empirical studies.

Laboratory experiments have been carried out to characterize equilibrium Cl-isotope fractionations between a few substances. Hoering and Parker (1961) equilibrated  $\text{Cl}_2$  and HCl at 296 K, measuring a fractionation of  $3.8 \pm 0.4\%$ . At this temperature, our calculated fractionation between  $\text{Cl}_2$  and HCl is  $2.7 \pm 0.4\%$ , not quite in agreement within the reported errors. The same authors measured a fractionation of  $0.9 \pm 0.3\%$  between HCl and crystalline  $\text{NH}_4\text{Cl}$  at 473 K, which can be crudely compared with our predicted fractionation of  $\sim 1.4 - 1.9\%$  between HCl and NaCl at the same temperature. Eggenkamp et al. (1995) measured fractionations between NaCl, KCl, and saturated brines. At 295 K, NaCl is  $0.3 \pm 0.1\%$  heavier than the coexisting NaCl-saturated brine, whereas KCl is  $0.1 \pm 0.1\%$  lighter than KCl-saturated brine. Our results predict that NaCl will be  $\sim 0.8\%$  heavier than coexisting KCl at this temperature. It is unclear what difference there might be in the isotopic behavior of a KCl brines and NaCl brines (both saturate at roughly 6 mol/L); there is likely to be some contact ion-pairing between solvated  $\text{M}^{+1}$  and  $\text{Cl}^-$  ions at these high solute concentrations (Jungwirth and Tobias, 2002). If we nonetheless assume that the two brines are identical (at least with respect to Cl-isotope partitioning), the Eggenkamp et al. (1995) result suggests a  $\sim 0.4\%$  fractionation between crystalline NaCl and KCl, which is in qualitative agreement with our theoretical calculation. By using the Eggenkamp et al. (1995) results, we can estimate that  $1000 \cdot \ln(\beta_{37-35}[\text{Brine}]) \approx 2.1 - 3.0$  at 295 K ( $22^\circ\text{C}$ ) for brines where NaCl or KCl is the dominant solute. We speculate that this may also serve as a rough estimate for the behavior of other aqueous chloride solutions, such as seawater and dilute hydrochloric acid, where  $\text{Cl}^-$  is coordinated largely or entirely by  $\text{H}_2\text{O}$  molecules.

Calculated fractionations can also be compared with the chlorine-isotope systematics observed in natural samples. One result of great interest is the predicted fractionation between NaCl- and KCl-saturated brines and the divalent-metal chlo-

rides  $\text{FeCl}_2$  and  $\text{MnCl}_2$ . If  $\text{FeCl}_2$  and  $\text{MnCl}_2$  are good analogues for structurally bound  $\text{Cl}^-$  in micas and amphiboles, our results suggest that, at equilibrium, these minerals will be  $\sim 2 - 3.5\%$  heavier than coexisting NaCl-dominated brines (at  $22^\circ\text{C}$ ). This agrees qualitatively with the observed systematics in hydrothermally altered oceanic crust (Magenheim et al., 1995), where Cl-bearing silicates have been found to be characteristically heavier than seawater, particularly for low-temperature minerals like smectite. Subduction-zone pore waters, which have strongly negative  $\delta^{37}\text{Cl}$  relative to seawater (Ransom et al., 1995), are also consistent with preferential retention or fixation of  $^{37}\text{Cl}$  in silicates. The bonding structure around dissolved  $\text{Cl}^-$  probably changes considerably as the temperature, pressure, and solute composition change, however, so it is not clear how to extrapolate our results for room-temperature NaCl- and KCl-saturated brines to other conditions of interest.

#### 4.3. Chlorine Isotopes, Groundwater Pollution, and Atmospheric Chlorine Cycling

Several of the studied molecular species are important in studies of groundwater pollution and atmospheric chlorine cycles. It is not clear that equilibrium fractionations will be observed in these natural systems, because of the importance of biological activity, slow reaction kinetics, and photochemistry. However, understanding the equilibrium fractionations underlying chemical transformations in these systems may help in designing and interpreting experiments on both natural systems and laboratory analogues. In this section we briefly relate our results to the isotopic systematics that have been observed in these systems.

Our results suggest that chlorine-bearing organic molecules will concentrate  $^{37}\text{Cl}$  relative to coexisting aqueous chloride or (at  $T \leq 400^\circ\text{C}$ ) gas-phase HCl. This result is of interest because chlorine-isotope measurements are being evaluated as a way of monitoring the remediation of chlorinated organic pollutants in groundwater (Sturchio et al., 1998; Heraty et al., 1999). In oxidizing groundwaters, it is thought that chlorinated organic molecules are destroyed via oxidation to inorganic species (i.e.,  $\text{CH}_2\text{Cl}_2 + \text{O}_2 \rightarrow \text{CO}_2 + 2\text{Cl}^-_{\text{aq}} + 2\text{H}^+_{\text{aq}}$ ).  $\text{Cl}^-_{\text{aq}}$  and HCl are both predicted to be isotopically light relative to coexisting organics like  $\text{CHCl}_3$  and  $\text{C}_2\text{HCl}_3$ , with equilibrium fractionations of 4.1 to 5.8‰ between the studied organics and HCl, and 5.8 to 8.5‰ between the studied organics and brine. The predicted equilibrium fractionations are quite large relative to observed fractionations. The largest measured fractionation,  $3.8 \pm 0.3\%$ , is observed during biologically mediated oxidation of  $\text{CH}_2\text{Cl}_2$  (Heraty et al., 1999). Our results suggest an equilibrium fractionation of  $\sim 6 - 7\%$  between  $\text{CH}_2\text{Cl}_2$  and brine at  $22^\circ\text{C}$ . Together, observations and theory suggest that oxidation reactions in the environment are not exhibiting equilibrium fractionation. Therefore, isotope fractionations in these systems may be sensitive to the details of reaction pathways and local biogeochemistry.

Chlorine-isotope reduced partition function ratios have been calculated for the most abundant Cl-bearing atmospheric molecules (HCl, ClO, and  $\text{ClONO}_2$ ), as well as a number of other species that are of interest in particular atmospheric reactions (i.e.,  $\text{Cl}_2$ ,  $\text{ClNO}_2$ ). One potential application of these results is to the study of Cl-volatilization from marine aerosols. In two

previous studies (Volpe and Spivack, 1994; Volpe et al., 1998), measured  $\delta^{37}\text{Cl}$  was compared with solute compositions for suites of marine aerosol particles collected on Bermuda and in the central equatorial Pacific. In the largest size-fractions among collected Pacific aerosols,  $\delta^{37}\text{Cl}$  decreases with increasing chlorine loss (as indicated by high Na/Cl ratios), and Volpe et al. (1998) suggest this is the result of rapid cycling of Cl between aerosols and a gas-phase reservoir; they infer a 2.8 to 3.0‰ fractionation between the gas-phase reservoir and the aerosol chloride. The calculated equilibrium fractionation between HCl and brine is  $\sim 1.7$  to 2.6‰ at 295 K, quite close to their inferred fractionation. This suggests that HCl may indeed dominate a gas-phase reservoir that reaches exchange equilibrium with large aerosols. Volpe and Spivack (1994) suggest that the fractionation observed in aerosol evaporation experiments (and in small natural aerosols), which goes in the opposite direction than the fractionation observed in large aerosols, is probably fundamentally kinetic. This is consistent with our results, because neither HCl nor any other plausible Cl-bearing vapor species (except monoatomic Cl) will be  $^{37}\text{Cl}$ -depleted relative to a saturated NaCl brine.

## 5. CONCLUSIONS

Equilibrium chlorine-isotope ( $^{37}\text{Cl}/^{35}\text{Cl}$ ) fractionations have been investigated by using published vibrational spectra and force-field modeling to calculate reduced partition function ratios for Cl-isotope exchange. Calculated fractionations are mainly controlled by the oxidation state of Cl and its bond partners. Molecular mass also appears to play a role in determining relative fractionations among simple Cl-bearing organic species. Molecules and complexes with oxidized Cl (i.e.,  $\text{Cl}^0$ ,  $\text{Cl}^{+1}$ ,  $\text{Cl}^{+2}$ , etc.) will concentrate  $^{37}\text{Cl}$  relative to chlorides (substances with  $\text{Cl}^-$ ). Among chlorides, heavy chlorine will be concentrated in substances where Cl is bonded to +2 cations (i.e.,  $\text{FeCl}_2$ ,  $\text{MnCl}_2$ , micas, and amphiboles) relative to substances where Cl is bonded to +1 cations (NaCl, KCl, and RbCl); organic molecules with C-Cl bonds will be heavier still. The experiments of Eggenkamp et al. (1995), in combination with our results, suggest that silicates (to the extent they are analogous with  $\text{FeCl}_2$  and  $\text{MnCl}_2$ ) will have higher  $^{37}\text{Cl}/^{35}\text{Cl}$  ratios than coexisting brine, by  $\sim 2$ –3‰ at room temperature. Calculated fractionations between HCl and  $\text{Cl}_2$ , and between brines and alteration minerals (mica and amphibole), are in qualitative agreement with experimental results and systematics observed in natural samples. Our results suggest that Cl-bearing organic molecules will have markedly higher  $^{37}\text{Cl}/^{35}\text{Cl}$  ratios (by 5.8‰ to 8.5‰ at 295 K) than coexisting aqueous solutions at equilibrium. In addition, our results are consistent with the presence of an isotopically heavy reservoir of HCl in exchange equilibrium with  $\text{Cl}^-_{\text{Aq}}$  in large marine aerosols, as inferred by Volpe et al. (1998).

*Acknowledgments*—We thank Juske Horita and several anonymous reviewers for their insightful and constructive comments on the article in manuscript. We would also like to thank Max Coleman and Elizabeth Johnson for helpful discussions during the early stages of this study. E.A.S. is grateful to have first learned to use a mass spectrometer in Robert Clayton's lab at the University of Chicago, and we are honored to be able to contribute to a special volume celebrating Dr. Clayton's outstanding contributions to experimental and theoretical stable isotope geochemistry. This study was funded in part by the

National Science Foundation, grants EAR-0106696 to H.P.T. and E.A.S. and EAR-0125767 to G.R.R. California Institute of Technology Division of Geological and Planetary Sciences Contribution 8934.

Associate editor: J. Horita

## REFERENCES

- Abel B., Hamann H. H., Kachanov A. A., and Troe J. (1995) Intracavity laser absorption spectroscopy of HOCl overtones. I. The  $3\nu_1 + 2\nu_2$  band and numbers of vibrational states. *J. Chem. Phys.* **104**(9), 3189–3197.
- Benedek G. and Frey A. (1980) Lattice dynamics of layered transition-metal dihalides. *Phys. Rev. B*, **21**, 2482–2498.
- Bigeleisen J. and Mayer M. G. (1947) Calculation of equilibrium constants for isotopic exchange reactions. *J. Chem. Phys.* **15**, 261–267.
- Black G. M. and Law M. M. (2001) The general harmonic force field of methyl chloride. *J. Mol. Spectrosc.* **205**, 280–285.
- Burkholder J. B., Hammer P. D., Howard C. J., Maki A. G., Thompson G., and Chackerian C. J. (1987) Infrared measurements of the ClO radical. *J. Mol. Spectrosc.* **124**, 139–161.
- Castro J. B. and Anaconda J. R. (1994) Normal-coordinate analysis and Coriolis coupling constants of ethylene type molecules,  $\text{C}_2\text{X}_4$  ( $\text{X} = \text{F}, \text{Cl}, \text{Br}, \text{I}$ ). *J. Mol. Struct.* **304**, 273–278.
- Chabanel M., Legoff D., and Touaj K. (1996) Aggregation of perchlorates in aprotic donor solvents Part 1.—Lithium and sodium perchlorates. *J. Chem. Soc. Faraday Trans.* **92**, 4199–4205.
- Clark R. J. H., Ellestad O. H., and Escribano R. (1976) The vapour phase Raman spectra, Raman band contour analyses, Coriolis coupling constants, and force constants for the molecules  $\text{F}^{12}\text{CH}_3$ ,  $\text{F}^{13}\text{CH}_3$ ,  $\text{H}^{12}\text{CCl}_3$ , and  $\text{H}^{13}\text{CCl}_3$ . *Mol. Phys.* **31**, 65–81.
- Clyne M. A. A. and Coxon J. A. (1970) The visible band absorption spectrum of chlorine. *J. Mol. Spectrosc.* **33**, 381–406.
- Copley J. R. D., MacPherson R. W., and Timusk T. (1969) Lattice dynamics of potassium chloride. *Phys. Rev.* **182**, 965–972.
- Decius J. F. and Murhammer D. (1980) Absolute i.r. intensities, dipole derivatives, and vibrational charge parameters in the perchlorate anion. *Spectrochim. Acta* **36A**, 965–969.
- Duncan J. L., Lawie D. A., Nivellini G. D., Tullini F., Ferguson A. M., Harper J., and Tonge K. H. (1987) The empirical general harmonic force-field of methylene-chloride. *J. Mol. Spectrosc.* **121**(2), 294–303.
- Duxbury G. and McPheat R. (1995) High-resolution absorption spectrum of the  $\nu_2$  band of nitryl chloride,  $\text{ClNO}_2$ , at  $793\text{ cm}^{-1}$ . *J. Mol. Spectrosc.* **174**, 446–458.
- Eastoe C. J., Long A., and Knauth L. P. (1999) Stable chlorine isotopes in the Palo Duro Basin, Texas: Evidence for preservation of Permian evaporite brines. *Geochim. Cosmochim. Acta* **63**, 1375–1382.
- Eggenkamp H. G. M., Kreulen R., and Van Groos A. F. K. (1995) Chlorine stable isotope fractionation in evaporites. *Geochim. Cosmochim. Acta* **59**, 5169–5175.
- Elcombe M. M. and Hulston J. R. (1975) Calculation of sulphur isotope fractionation between sphalerite and galena using lattice dynamics. *Earth Planet. Sci. Lett.* **28**, 172–180.
- Escribano R., Orza J. M., Montero S., and Domingo C. (1979) Absolute Raman intensities, force constants, and electro-optical parameters of  $\text{CH}_2\text{Cl}_2$ ,  $\text{CD}_2\text{Cl}_2$ , and  $\text{CHDCl}_2$ . *Mol. Phys.* **37**, 361–377.
- Escribe C., Bouillot J., and Ziebeck K. R. A. (1980) Lattice dynamics of  $\text{MnCl}_2$ . *J. Phys. C Solid State Phys.* **13**, 4053–4060.
- Gale J. D. (1997) GULP—A computer program for the symmetry adapted simulation of solids. *J. Chem. Soc. Faraday Trans.* **93**, 629–637.
- Hanschmann G. (1984) Reduzierte Zustandssummenverhältnisse isotope Moleküle auf quantenchemischer Grundlage V. Mitt. MNDOMO-Berechnungen zur  $^{28}\text{Si}/^{30}\text{Si}$ -,  $^{32}\text{S}/^{34}\text{S}$ - und  $^{35}\text{Cl}/^{37}\text{Cl}$ -Substitution. *Isotopenpraxis* **12**, 437–439.
- Heraty L. J., Fuller M. E., Huang L., Abrajano T. J., and Sturchio N. C. (1999) Isotopic fractionation of carbon and chlorine by microbial degradation of dichloromethane. *Org. Geochem.* **30**, 793–799.

- Hoering T. C. and Parker P. L. (1961) The geochemistry of the stable isotopes of chlorine. *Geochim. Cosmochim. Acta* **23**, 186–199.
- Huang L., Sturchio N. C., Abrajano T. J., Heraty L. J., and Holt B. D. (1999) Carbon and chlorine isotope fractionation of chlorinated aliphatic hydrocarbons by evaporation. *Org. Geochem.* **30**, 777–785.
- Jendzrejewski N., Eggenkamp H. G. M., and Coleman M. L. (2001) Characterisation of chlorinated hydrocarbons from chlorine and carbon isotopic compositions: Scope of application to environmental problems. *Appl. Geochem.* **16**, 1021–1031.
- Jones L. H., Swanson B. I., and Ekberg S. A. (1984) Isotope shifts and force field for carbon tetrachloride in a krypton matrix. *J. Phys. Chem.* **88**, 5560–5563.
- Jungwirth P. and Tobias D. J. (2002) Ions at the air/water interface. *J. Phys. Chem. B* **106**, 6361–6373.
- Kaufmann R., Long A., Bentley H., and Davis S. (1984) Natural chlorine isotope variations. *Nature* **309**, 338–340.
- Kieffer S. W. (1982) Thermodynamics and lattice vibrations of minerals: 5. Applications to phase equilibria, isotopic fractionation, and high-pressure thermodynamic properties. *Rev. Geophys. Space Phys.* **20**, 827–849.
- King S. T. (1968) Infrared study of matrix-isolated chlorinated tetrahedral molecules. *J. Chem. Phys.* **49**, 1321–1330.
- Kisiel Z. and Pyszczkowski L. (1996) Assignment and analysis of the mm-wave rotational spectrum of trichloroethylene: Observation of a new, extended <sup>2</sup>R-band and an overview of high-*J*, *R*-type bands. *J. Mol. Spectrosc.* **178**, 125–137.
- Kotaka M. and Kakahana H. (1977) Thermodynamic isotope effect of trigonal planar and tetrahedral species. *Bull. Res. Lab Nuc. Reactors* **2**, 13–29.
- Kotaka M., Shono T., Ikuta E., and Kakahana H. (1978) Thermodynamic isotope effect of some octahedral hexahalo complexes. *Bull. Res. Lab Nuc. Reactors* **3**, 31–37.
- Long A., Eastoe C. J., Kaufmann R. S., Martin J. G., Wirt L., and Finley J. B. (1993) High-precision measurement of chlorine stable isotope ratios. *Geochim. Cosmochim. Acta* **57**, 2907–2912.
- Magenheim A. J., Spivack A. J., Michael P. J., and Gieskes J. M. (1995) Chlorine stable isotope composition of the oceanic crust: Implications for Earth's distribution of chlorine. *Earth Planet. Sc. Lett.* **131**, 427–432.
- Makino K. and Tomita K. (1993) Effect of chlorine on the crystal structure of a chlorine-rich hastingsite. *Mineral. Mag.* **57**, 677–685.
- Mohan N. and Müller A. (1972) Determination of the exact force-field of SiCl<sub>4</sub> from <sup>35</sup>Cl-<sup>37</sup>Cl isotope shift and analysis of the vibrational spectra of Si<sup>35</sup>Cl<sub>3</sub>Cl, Si<sup>35</sup>Cl<sub>2</sub><sup>37</sup>Cl<sub>2</sub>, Si<sup>35</sup>Cl<sup>37</sup>Cl<sub>3</sub>, <sup>28</sup>SiCl<sub>4</sub>, <sup>29</sup>SiCl<sub>4</sub>, and <sup>30</sup>SiCl<sub>4</sub>. *J. Mol. Spectrosc.* **42**, 203–207.
- Müller H. S. P., Helminger P., and Young S. H. (1997a) Millimeter and submillimeter spectroscopy of chlorine nitrate: The Cl quadrupole tensor and the harmonic force field. *J. Mol. Spectrosc.* **181**, 363–378.
- Müller H. S. P., Sorensen G. O., Birk M., and Friedl R. R. (1997b) The rotational spectrum and anharmonic force field of chlorine dioxide, OClO. *J. Mol. Spectrosc.* **186**, 177–188.
- Müller H. S. P. and Willner H. (1993) Vibrational and electronic spectra of chlorine dioxide, OClO, and chlorine superoxide, ClOO, isolated in cryogenic matrices. *J. Phys. Chem.* **97**, 10589–10598.
- Nakamoto, K. (1997). *Infrared and Raman Spectra of Inorganic and Coordination Compounds*. Wiley.
- Nilsson G. G. (1979) Phonon frequencies in off-symmetry directions of NaCl determined by neutron inelastic scattering. *Phys. Stat. Sol. B* **91**, 83–86.
- Oberti R., Ungaretti L., Cannillo E., and Hawthorne F. C. (1993) The mechanism of Cl incorporation in amphibole. *Am. Mineral.* **78**, 746–752.
- Orphal J., Morillon-Chapey M., Diallo A., and Guelachvili G. (1997) High-resolution infrared spectra and harmonic force field of chlorine nitrate. *J. Phys. Chem. A* **101**, 1062–1067.
- Orphal J., Morillon-Chapey M., Klee S., Mellau G. C., and Winnewisser M. (1998) The far-infrared spectrum of ClNO<sub>2</sub> studied by high-resolution Fourier-transform spectroscopy. *J. Mol. Spectrosc.* **190**, 101–106.
- Parekunnel T., Hirao T., Le Roy R. J., and Bernath P. F. (1999) FTIR emission spectra and molecular constants for DCl. *J. Mol. Spectrosc.* **195**, 185–191.
- Parrington J. R., Knox H. D., Breneman S. L., Baum E. M., and Feiner F. (1996). *Chart of the Nuclides*. General Electric Co. and KAPL Inc.
- Pople J. A., Scott A. P., Wong M. W., and Radom L. (1993) Scaling factors for obtaining fundamental vibrational frequencies and zero-point energies from HF/6-31G\* and MP2/6-31G\* harmonic frequencies. *Israel J. Chem.* **33**, 345–350.
- Ransom B., Spivack A. J., and Kastner M. (1995) Stable Cl isotopes in subduction-zone pore waters: Implications for fluid-rock reactions and the cycling of chlorine. *Geology* **23**, 715–718.
- Raunio G. and Almqvist L. (1969) Dispersion relations for phonons in KCl at 80 and 300 K. *Phys. Stat. Sol.* **33**, 209–215.
- Raunio G., Almqvist L., and Stedman R. (1969) Phonon dispersion relations in NaCl. *Phys. Rev.* **178**, 1496–1501.
- Raunio G. and Rolandson S. (1970a) Lattice dynamics of NaCl, KCl, RbCl, and RbF. *Phys. Rev. B* **2**, 2098–2103.
- Raunio G. and Rolandson S. (1970b) Phonon dispersion relations in RbCl and RbF at 80 K. *J. Phys. C Solid State Phys.* **3**, 1013–1025.
- Richet P., Bottinga Y., and Javoy M. (1977) A review of hydrogen, carbon, nitrogen, oxygen, sulphur, and chlorine stable isotope fractionation among gaseous molecules. *Ann. Rev. Earth Planet. Sci.* **5**, 65–110.
- Rochekind M. M. and Pimentel G. C. (1965) Infrared spectrum and vibrational assignment for chlorine monoxide, Cl<sub>2</sub>O. *J. Chem. Phys.* **42**, 1361–1368.
- Schauble E. A., Rossman G. R., and Taylor H. P. Jr. (2001) Theoretical estimates of equilibrium Fe-isotope fractionations from vibrational spectroscopy. *Geochim. Cosmochim. Acta* **65**, 2487–2497.
- Schmidt K. H. and Müller A. (1974) Vibrational spectrum of H<sup>13</sup>CCl<sub>3</sub> and the force field of chloroform. *J. Mol. Spectrosc.* **50**, 115–125.
- Schmidt M. W., Baldrige K. K., Boatz J. A., Elbert S. T., Gordon M. S., Jensen J. J., Koseki S., Matsunaga N., Nguyen K. A., Su S., Windus T. L., Dupuis M., and Montgomery J. A. (1993) General atomic and molecular electronic-structure system. *J. Comput. Chem.* **14**, 1347–1363.
- Schmunk R. E. and Winder D. R. (1970) Lattice dynamics of sodium chloride at room temperature. *J. Phys. Chem. Solids* **31**, 131–141.
- Schnöckel H. G. and Becher H. J. (1975) <sup>35</sup>Cl/<sup>37</sup>Cl-verschiebungen in den infrarotspektren von matrixisoliertem tetrachloräthylen und phosgen und ihre auswertung in der kraftkonstantenberechnung. *J. Mol. Struct.* **25**, 369–376.
- Schrader B., Meier W. (1974). *DMS Raman/IR Atlas of Organic Compounds*. Verlag Chemie GmbH.
- Scott A. P. and Radom L. (1996) Harmonic vibrational frequencies: An evaluation of Hartree-Fock, Møller-Plesset, quadratic configuration interaction, density functional theory, and semiempirical scale factors. *J. Phys. Chem.* **100**, 16502–16513.
- Snels M., D'Amico G., Piccarreta L., Hollenstein H., and Quack M. (2001) Diode-laser jet spectra and analysis of the ν<sub>1</sub> and ν<sub>4</sub> fundamentals of CCl<sub>3</sub>F. *J. Mol. Spectrosc.* **205**, 102–109.
- Sturchio N. C., Clausen J. L., Heraty L. J., Huang L., Holt B. D., and Abrajano T. J. (1998) Chlorine isotope investigation of natural attenuation of trichloroethene in an aerobic aquifer. *Environ. Sci. Technol.* **32**(20), 3037–3042.
- Tanaka H. and Hisano K. (1989) A far-infrared emission study on the phonon self-energy of KCl at high temperature. *J. Phys. Condens. Matter* **1**, 9539–9545.
- Urey H. C. (1947) The thermodynamic properties of isotopic substances. *J. Chem. Soc.*, 562–581.
- Urey H. C. and Greiff L. J. (1935) Isotopic exchange equilibria. *J. Am. Chem. Soc.* **57**, 321–327.
- Vengosh A., Chivas A. R., and McCulloch M. T. (1989) Direct determination of boron and chlorine isotopic compositions in geological materials by negative thermal-ionization mass spectrometry. *Chem. Geol.* **79**, 333–343.
- Vettier C. and Yelon W. B. (1975) The structure of FeCl<sub>2</sub> at high pressures. *J. Phys. Chem. Solids* **36**, 401–405.
- Volfinger M., Robert J.-L., Vielzeuf D., and Neiva A. M. R. (1985) Structural control of the chlorine content of OH-bearing silicates (micas and amphiboles). *Geochim. Cosmochim. Acta* **49**, 37–48.
- Volpe C. and Spivack A. J. (1994) Stable chlorine isotopic composition of marine aerosol particles in the western Atlantic Ocean. *Geophys. Res. Lett.* **21**(12), 1161–1164.
- Volpe C., Wahlen M., Pszeny A. A. P., and Spivack A. J. (1998)

- Chlorine isotopic composition of marine aerosols: Implications for the release of reactive chlorine and HCl cycling rates. *Geophys. Res. Lett.* **25**(20), 3831–3834.
- Wakamura K. (1993) Thermal expansion and anharmonic phonon–phonon interaction effects on an effective charge in GaAs and KCl. *J. Phys. Chem. Solids* **54**(3), 387–395.
- Wong M. W. (1996) Vibrational frequency prediction using density functional theory. *Chem. Phys. Lett.* **256**, 391–399.
- Xiao Y.-K. and Zhang C.-G. (1992) High precision isotopic measurement of chlorine by thermal ionization mass spectrometry of the  $\text{Cs}_2\text{Cl}^+$  ion. *Intl. J. Mass Spectrom. Ion Proc.* **116**, 183–192.
- Xu Y., McKellar A. R. W., Burkholder J. B., and Orlando J. J. (1996) High-resolution infrared spectrum of the  $\nu_1$  and  $\nu_3$  bands of dichlorine monoxide,  $\text{Cl}_2\text{O}$ . *J. Mol. Spectrosc.* **175**, 68–72.
- Yelon W. B., Scherm R., and Vettier C. (1974) Acoustic phonon spectra of  $\text{FeCl}_2$ . *Solid State Commun.* **15**, 391–394.